Government of **Western Australia**
Department of **Mines, Industry Regulation and Safety**

RECORD 2019/7

A SYN-DEPOSITIONAL SILL INTRUSIVE MODEL FOR THE GOLDEN MILE DOLERITE, KALGOORLIE, WESTERN AUSTRALIA

by
RM McMann

Geological Survey of Western Australia

CODES
CENTRE FOR ORE DEPOSIT AND EARTH SCIENCES
UNIVERSITY of TASMANIA
AUSTRALIA

Government of **Western Australia**
Department of **Mines, Industry Regulation and Safety**

RECORD 2019/7

A SYN-DEPOSITIONAL SILL INTRUSIVE MODEL FOR THE GOLDEN MILE DOLERITE, KALGOORLIE, WESTERN AUSTRALIA

by
RM McMann

PERTH 2019

Geological Survey of Western Australia

MINISTER FOR MINES AND PETROLEUM
Hon Bill Johnston MLA

DIRECTOR GENERAL, DEPARTMENT OF MINES, INDUSTRY REGULATION AND SAFETY
David Smith

EXECUTIVE DIRECTOR, GEOLOGICAL SURVEY AND RESOURCE STRATEGY
Jeff Haworth

REFERENCE
The recommended reference for this publication is:
McMann, RM 2019, A syn-depositional sill intrusive model for the Golden Mile Dolerite, Kalgoorlie, Western Australia: Geological Survey of Western Australia, Record 2019/7, 93p.

ISBN 978-1-74168-850-4
ISSN 2204-4345

Grid references in this publication refer to the Geocentric Datum of Australia 1994 (GDA94). Locations mentioned in the text are referenced using Map Grid Australia (MGA) coordinates, Zone 50. All locations are quoted to at least the nearest 100 m.

CODES
CENTRE FOR ORE DEPOSIT AND EARTH SCIENCES

UNIVERSITY of TASMANIA
AUSTRALIA

Published 2019 by the Geological Survey of Western Australia
This Record is published in digital format (PDF) and is available online at <www.dmp.wa.gov.au/GSWApublications>.

Further details of geoscience products and maps are available from:
Information Centre
Department of Mines, Industry Regulation and Safety
100 Plain Street
EAST PERTH WESTERN AUSTRALIA 6004
Telephone: +61 8 9222 3459 Facsimile: +61 8 9222 3444
www.dmp.wa.gov.au/GSWApublications

Cover image: Sunset over the Yalgoo Mineral Field. Photograph by T Ivanic, DMIRS

A syn-depositional sill intrusive model for the Golden Mile Dolerite, Kalgoorlie, Western Australia

By

Ryan Michael McMann

Supervised by: Professor Raymond Cas and Dr Paul Olin

UNIVERSITY OF TASMANIA

Submitted in fulfilment of the requirements for the degree of Bachelor of Science with Honours in Economic Geology

University of Tasmania, May 2018

Declaration of originality

This thesis contains no material which has been accepted for the award of any other degree or diploma in any tertiary institution and, to the best of my knowledge and belief, contains no copy or paraphrase of material previously published or written by another person, except where due reference is made in the text of this thesis.

Signature:_____ Date:_____

Abstract

The Golden Mile Dolerite Kalgoorlie Western Australia is host to one of Australia's largest and most famous greenstone gold deposits. Despite being studied and mined for over 100 years the Golden Mile Dolerite still sparks controversy within industry and the academic community with regards to its mode of emplacement. This study aimed to investigate the two main emplacement theories of widely accepted post-depositional intrusive sill (Travis et al., 1971, Bateman et al., 2001) to the less popular, at least partially extrusive origin (Tomich, 1974, Golding, 1985). The Golden Mile Dolerite is a thick (850m) tholeiitic, heavily differentiated Archean mafic body which shows a range of textures from fine marginal basalts to coarse gabbroic sections as well as locally isolated and massive granophyric segregations.

Observations made on the contact relationships through the detailed graphic logging of four recently drilled stratigraphic diamond drillholes between the Golden Mile Dolerite (GMD) and the surrounding sediments of the Black Flag Group. These observations were particularly concerned with mudstone matrix supported angular basaltic breccia which appeared within the black mudstone on the basaltic margins of mafic bodies. The detailed graphic logging was accompanied by down hole, whole rock geochemical analysis of two of the studied drill holes to investigate the internal geochemical trends of the GMD. These breccias have been interpreted as hyaloclastite fragments forming peperitic margins through magma wet-unconsolidated magma interaction. When paired with whole rock geochemical data the recognition of at least two magmatic pulses can be seen within the thicker section of the GMD. The combined observations of this study suggest that the Golden Mile Dolerite is likely a high level syn-intrusive sill which has intruded the black mudstones of the Black Flag Group, during or shortly after their deposition.

Acknowledgments

Firstly, I would like to acknowledge and thank the Geological Survey of Western Australia, for their extensive support of this project. Through not only in the funding of this research and the use of their core facilities, but also the help offered by the staff of the core library and the knowledge and support of the survey's geologists. I would like to personally thank Debbie Caple for helping me navigate the sampling process and the associated government forms. I would also like to thank the core technicians for their exemplary work. The advice and geological support offered by Jyotindra Sapkota during my time spent logging core in was very reassuring for not having log much core before that point. The geochemical sampling of JUGD011 and SE18 which gave a lot of insight into the internal processes of the Golden Mile Dolerite would not have been possible without a generous offer to process the collected samples by Hugh Smithies for which I am incredibly grateful.

I would also like to thank KCMG for allowing me access to drill hole TRGD001 as well as going above and beyond by having it shipped to the GSWA core library.

The advice, support and extensive geological knowledge offered by my primary supervisor Ray Cas both in the field and throughout the year through both corrections and conversations were greatly appreciated. The opportunity to see some spectacular volcanic exposures on the east coast of Australia during his volcanology course was a highlight of the project, as well as introducing me to the wonderful drink that is Tooheys Old. This project has been a great experience and I have learned a lot and would like to thank you again for offering this project and giving me the chance to participate in it

To Paul my secondary/Co-supervisor, thanks for always being willing to stop and have a chat in the hallway about geology or pretty much anything else that was going on at the time. These conversations were great for running sometimes questionable ideas past you first before sending them to Ray and almost always helped with the inevitable stresses of honours.

I would like to thank all of the UTas staff for their support both great and small. To my fellow midyear honours students, the friendships we have made during undergrad and the last nine months have been way better than I could have ever expected. Your support and friendship made this degree worth it, I hope you all the best in your future endeavours and will hopefully see you on a mine site before too long.

Finally, I would like to thank my family for their continued love and support during this last nine months, I wouldn't have been able to do it without you. In particular I would like to thank my cousin Dr Loren Oschipok for getting me interested in science as a kid and inspiring me continue with further education.

TABLE OF CONTENTS

List of figures

2.0. Regional geology

4.0. Lithofacies of the Kalgoorlie area

5.0. Geochemistry

6.0. **Discussion**

List of appendices

1.0. Introduction

1.1. The controversy of the Golden Mile Dolerite: how was it emplaced?

Despite the Late Archean Golden Mile Dolerite, Kalgoorlie, Western Australia, being studied and mined for over 100 years, there is still discussion with regards to its mode of emplacement. This discussion focuses on whether or not the GMD is either a very thick, ponded, basaltic lava flow or, as is more widely accepted, a strongly differentiated dolerite sill. Supposed evidence supporting both theories have been presented and used to strongly support each hypothesis by the researchers who have proposed them. Newly acquired evidence presented in this study will add to the ongoing discussion, with the aim of suggesting new interpretations of the GMD and its method of emplacement.

1.2. Mining history and location

Kalgoorlie, Western Australia, is host to one of Australia's largest and most famous gold mines, the Fimiston Open Pit or more colloquially known as the Kalgoorlie or KCGM Super Pit. It is located in the Kambalda domain of the Kalgoorlie Terrane in the south-west of the Eastern Goldfields Superterrane, approximately 549 km east of Perth. The Fimiston Open Pit was the largest operating open pit mine in Australia until 2016, when it was surpassed by the Newmont, Boddington goldmine open pit in WA. From its discovery in 1893 By Dan Shea, Paddy Hannan and Tom Flanagan, the approximately 3.8Km stretch of land known as the Golden Mile has produced over 58 million ounces of gold (Nixon et al., 2014). The majority of this gold has come from mineralization of the aptly named Archean Golden Mile Dolerite, with the highest recorded production occurring in 1903 producing 1,012,151 ounces of gold (Travis et al., 1971).

1.3. Deposit mineralization

The Golden Mile Dolerite is a thick tholeiitic unit with variations in grain size from fine basalt through to coarse gabbro and areas of granophyre thought to be the result of differentiation within the melt (Travis et al., 1971). The GMD acts as the primary host for the Fimiston mine in which mineralization is controlled in several lode systems as described by Swager (1989). The main lodes consist of two groups of steeply dipping lode systems,

the Eastern and Western loads which occur on the either side of the Golden Mile Fault. Mineralization on the contact between the Paringa Basalt and the GMD through a series of shallow dipping lodes has also been mined at economic grades. Gold is hosted in these lodes in several mineral states, these include gold tellurides, free gold and pyrite hosted in wall rock (Mueller et al., 1988, Mueller, 2015, Vielreicher et al., 2010).

1.4. The importance of contact relationships in understanding emplacement mechanisms

Understanding the contact relationships and textures in mafic igneous rock units is incredibly important in determining the environment and mode(s) of emplacement. This, however, can be very difficult to determine in outcrop or hand sample; for example, basalt in a lava flow may have the same texture and chemistry as an intrusive basaltic body. Due to these similarities, to correctly differentiate between an intrusive and extrusive package a complete view of the unit is needed, or at the very least of the top contact. Other features such as chemical differentiation and crystal size can be used to infer an origin but are not always reliable. The presence of a well-defined top contact is the best indicator, though at times this may be obscured by alteration or through faulting or post-emplacement erosional processes.

A common texture of deep intrusive bodies into solid rock is the presence of relatively planar or cross-cutting boundary with the host rock which it intrudes (Marsh, 2015). In contrast, shallow intrusive bodies which intrude into sedimentary basins may encounter unconsolidated, often water-saturated sediments. At the sediment-magma contact quench fragmentation occurs which leads to a mixing of igneous hyaloclast fragments into the host sediments as the sediment pore water is heated and convects vigorously (Kokelaar, 1982, van Otterloo et al., 2015b, White et al., 2000, McPhie and Cas, 2015, McPhie, 1993). The resulting sediment-hyaloclast mixture, called peperite, is a strong indicator of contemporaneous syn-depositional emplacement into the host sediments (Busby-Spera and White, 1987, White et al., 2000, McPhie et al., 1993). It can form around all margins of a syn-depositional intrusion, a can intrusive apophyses. In contrast, extrusive lavas, depending heavily on the environment into which they are extruded, may display a range of textures, including peperites and intrusive apophyses at bottom contacts, where burrowing into soft sediments can occur, but cannot have these features at the top contact because there is no

pre-existing sedimentary unit above the lava flow (McPhie et al., 1993, Marsh, 2015). An understanding of how to differentiate between intrusive and extrusive modes of emplacement is essential for developing the correct interpretation for the mode of emplacement of the Golden Mile Dolerite. This will play a vital role in the observations and inferences made in this thesis.

1.5. Previous research

The origin of the GMD has been a disputed topic since its discovery with debate continuing to the present day. Evidence for both intrusive and extrusive origins has been put forward and several theories currently exist, however, a post-depositional intrusive sill is currently the widely accepted model (O'Connor-Parsons and Stanley, 2007, Travis et al., 1971, McCall, 1973). This study will compare these theories to observations made through new detailed graphic logging of new and existing diamond drill holes and using newly acquired samples.

1.5.1. Intrusive origin

The Golden Mile Dolerite (GMD) described as the "younger greenstone" or quartz dolerite greenstone was suggested to be a sill or laccolith by Gustafson and Miller (1937). They suggest that the GMD had intruded between the overlying Black Flag beds and the underlying Paringa basalt whilst the units were flat lying. The intrusive origin theory has been supported by a number of subsequent studies (Travis et al., 1971, Bateman et al., 2001, McCall, 1973), with evidence focusing on significant variation in crystal sizes, geochemical layering and the presence of a granophyric zone (Travis et al., 1971, McCall, 1973, McDougall, 1962). Which was interpreted to suggest a large degree of differentiation associated with slow cooling rates, which normally are not seen in extrusive basalts (McPhie et al., 1993, McDougall, 1962, McDougall, 1964, Marsh, 2015). Textural units 1 and 10 as described by Travis et al. (1971) are thought to represent the lower and upper chilled margins of the sill respectively which are common features of intrusive bodies (Marsh, 2015).

1.5.2. Extrusive origin

A contesting theory for the formation of the Golden Mile Dolerite suggests that it was emplaced at least partially as an extrusive system. These claims are the result of observations regarding the relationships of the Golden Mile Dolerite with both the overlying Black Flag Beds and the underlying Paringa Basalt (Tomich, 1974, Golding, 1985). Supposed fragments of the Golden Mile Dolerite within the overlying volcaniclastic units of the Black Flag Beds has led to the interpretation of a flow top breccia that was eroded and through this fragments of GMD were mixed into the Black Flag Beds, suggesting that the GMD must have been a subaerial extrusive or deposited in a shallow subaqueous environment (Golding, 1985).

1.6 Aims

The aims of this study are:

1. Investigate the emplacement mechanism and environment of the Golden Mile Dolerite, through detailed graphic logging of recently acquired Geological Survey of Western Australia co-funded drill holes which intersect the distal extent of the Golden Mile Dolerite as well as comparing these with older holes, focusing on the contact relationships of the GMD.

2. To compare and define through petrography the variation in textures and mineralogy of the mafic Golden Mile Dolerite.

3. To observe geochemical trends within the Golden Mile Dolerite through samples taken from drill hole JUGD0011 and data supplied for drill hole SE18

2.0. Regional geology

2.1. Yilgarn Craton

The Yilgarn Craton is located in the southwest of Western Australia and is a large constituent of the western Australian Precambrian shield. The rocks of the Yilgarn Craton consist of metavolcanic, metasedimentary and granitic units including a series of greenstone belts which were primarily formed between 3050Ma and 2600Ma, as well as some rocks >3700 Ma (Czarnota et al., 2010). The Yilgarn Craton has been divided in numerous tectono-stratigraphic schemes based on different criteria, however, for this study, the terrane and domain scheme described by Cassidy et al. (2006) will be used (Fig. 2.1). The classification of these terrains is defined as "fault-bounded bodies of rock of regional extent, characterized by a geological history different to those adjacent to them" (Cassidy et al., 2006). Within the Craton six terranes have been described as seen in figure 2.1, including the South West, Narryer, Youanmi, Kalgoorlie, Kurnalpi and Burtville Terranes, and the Kalgoorlie, Kurnalpi and Burtville terranes can be amalgamated into the Eastern Goldfields Super Terrane (Cassidy et al., 2006). Each of these terranes has been subdivided into several domains (Cassidy et al., 2006). The western Yilgarn Craton, including the Narryer and Southwest terranes consists primarily of metamorphosed granites and granitic gneisses. In contrast, the Eastern Goldfields Superterrane and the central Youanmi Terrane contain broadly north trending greenstone belts separated by extensive granites, and volcanic, sedimentary and granitic gneisses (Czarnota et al., 2010, Squire et al., 2010).

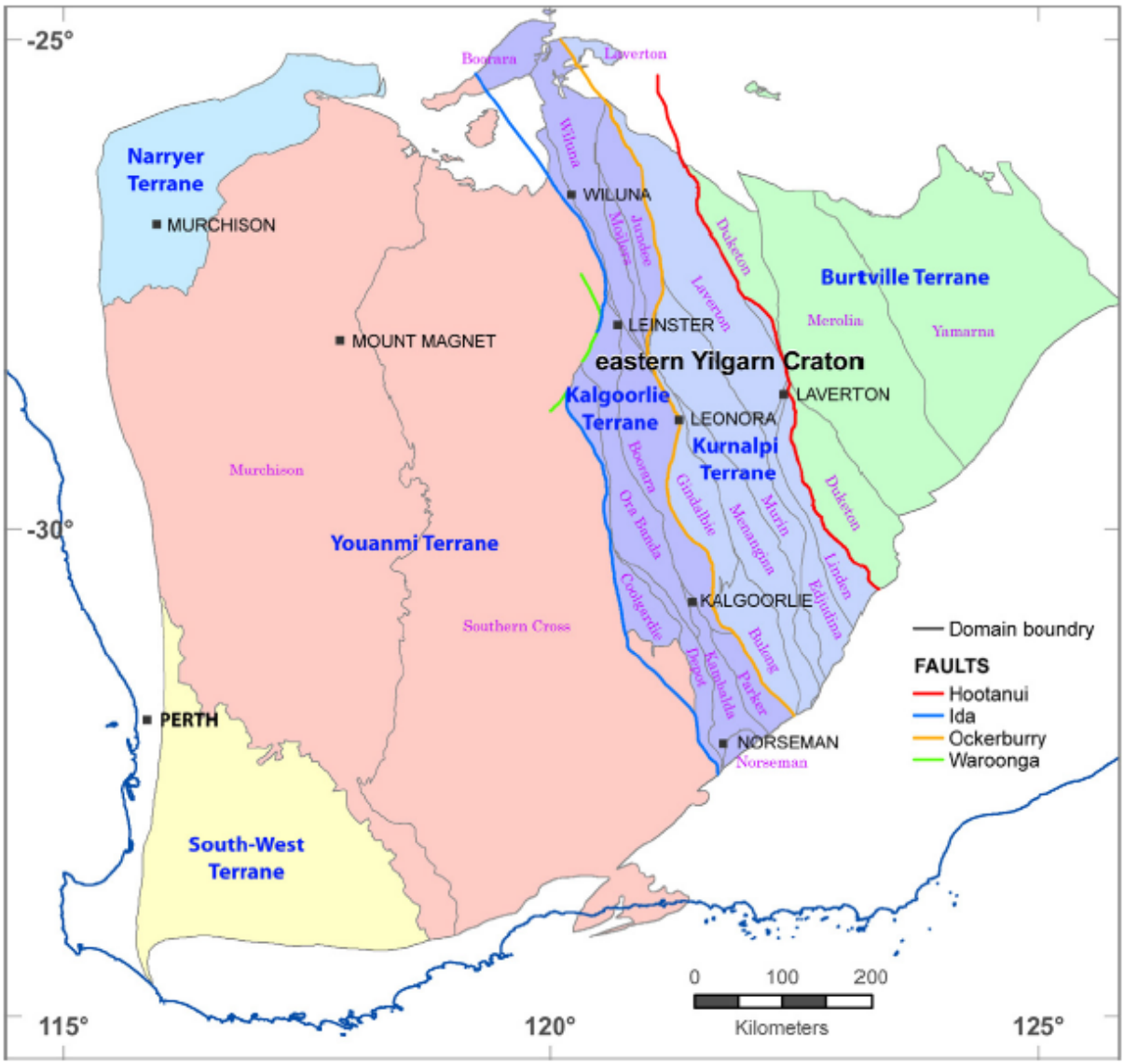

Figure 2.1 Map of the terranes and domains of the Yilgarn Craton from Czarnota et al. (2010)

2.2. Eastern Goldfields Superterrane

The Eastern Goldfields Superterrane consists of the amalgamation of three terranes, these include the Kalgoorlie, Burtville, and Kurnalpi. Each of these three terranes has been defined on their own unique volcanic facies, geochemistry and periods of volcanic activity which span from approximately 2940Ma to 2660Ma (Czarnota et al., 2010). These elongated terranes are separated by a series of roughly NNW trending regional scale faults (Swager, 1997). The greenstone belts of the Eastern Goldfields Superterrane can be classified into four distinct subgroups based on their relative time of emplacement, these being 2940, 2810,

2760 and 2715-2620 Ma (Czarnota et al., 2010). Czarnota et al. (2010) link these periods of greenstone formation or emplacement to work done by Cassidy et al. (2004) implying that the emplacement of greenstones and granitic bodies at these times are related and represent periods of crustal growth. The rocks of the Eastern Goldfields Superterrane are thought to have primarily formed between 3050 and 2600Ma with rare occurrences of rocks containing zircon crystal fragments >3700 Ma old. Like the four greenstone forming events described by Czarnota et al. (2010) the majority of the volcaniclastic sequences observed in the Eastern Goldfields Superterrane formed during four main episodes of volcanism: approximately 2940Ma, 2810Ma, 2760Ma and 2715-2655Ma, occurring generally at the same time as greenstone formation (Squire et al., 2010). The mafic units of the greenstone belts of the Eastern Goldfields Superterrane are often overlain by thick sequences of more felsic Archean volcaniclastic sedimentary units. An example of this can be seen in the Kalgoorlie area where the GMD is found beneath the several km thick, Black Flag Group or Beds. These volcaniclastic units are thought to be the result of two major cycles of voluminous pyroclastic volcanism which end with extensive exhumation erosion as well as being linked to granite emplacement (Squire et al., 2010). The first of these cycles is thought to have occurred between 2690Ma and 2680Ma during which time the early and late Black Flag Group were emplaced. The second cycle which occurred approximately between 2670Ma and 2660Ma is thought to be similar in form to cycle one, however, a change in the composition of the volcaniclastic materials can be seen from the BFG and the unit formed during this later cycle, known as the Merougil Group (Squire et al., 2010).

Units formed during the 2940Ma, 2810Ma and 2760Ma intervals are exceedingly rare and often poorly preserved or exposed within the Eastern Goldfields Superterrane (Czarnota et al., 2010, Squire et al., 2010).

The only known rocks of the 2940Ma interval which remain preserved in the Eastern Goldfields Superterrane are the felsic volcanic rocks of the Penneshaw formation of the Kalgoorlie Terrane and those of the Mount Joanna and Dingo Range High Ca gneissic granites from the Burtville Terrane (Czarnota et al., 2010, Squire et al., 2010).

Examples of rocks originating from the 2810Ma period are more common than those seen in the 2940Ma and 2760Ma periods, however, they are still a volumetrically minor component of the Eastern Goldfields Superterrane. The rocks formed during this period can be seen across all three terranes and are primarily represented by tholeiitic pillow basalt, komatiites, banded iron formations as well as granites (Squire et al., 2010).

The 2760Ma period coincides with the deposition of the greenstones of the Merolia Domain of the Burtville Terrane, of which the rock record includes basaltic, komatiitic, felsic volcanic, shallow water sedimentary rocks and minor high Ca granites (Czarnota et al., 2010). During the period between 2760 Ma and 2715Ma minor events caused the production of sparse low volume mafic units which include units such as the Kathleen Valley Gabbro (Squire et al., 2010).

2.3. Kalgoorlie Terrane

The Kalgoorlie Terrane is subdivided into ten separate domains (Wiluna, Moilors, Jundee, Boorara, Orabanda, Coolgardie, Depot, Kambalda, Parker, and Norseman) (Cassidy et al., 2006). The study area of this project revolves around the northern extent of the Kambalda domain, and as a result, the descriptions of local geology will be focused on the area surrounding the town of Kalgoorlie (Figure 2.2). The geology of the Eastern Goldfields Superterrane is often referenced against the known stratigraphy of the Kalgoorlie Terrane, which in order of age (oldest to youngest) and formation are:

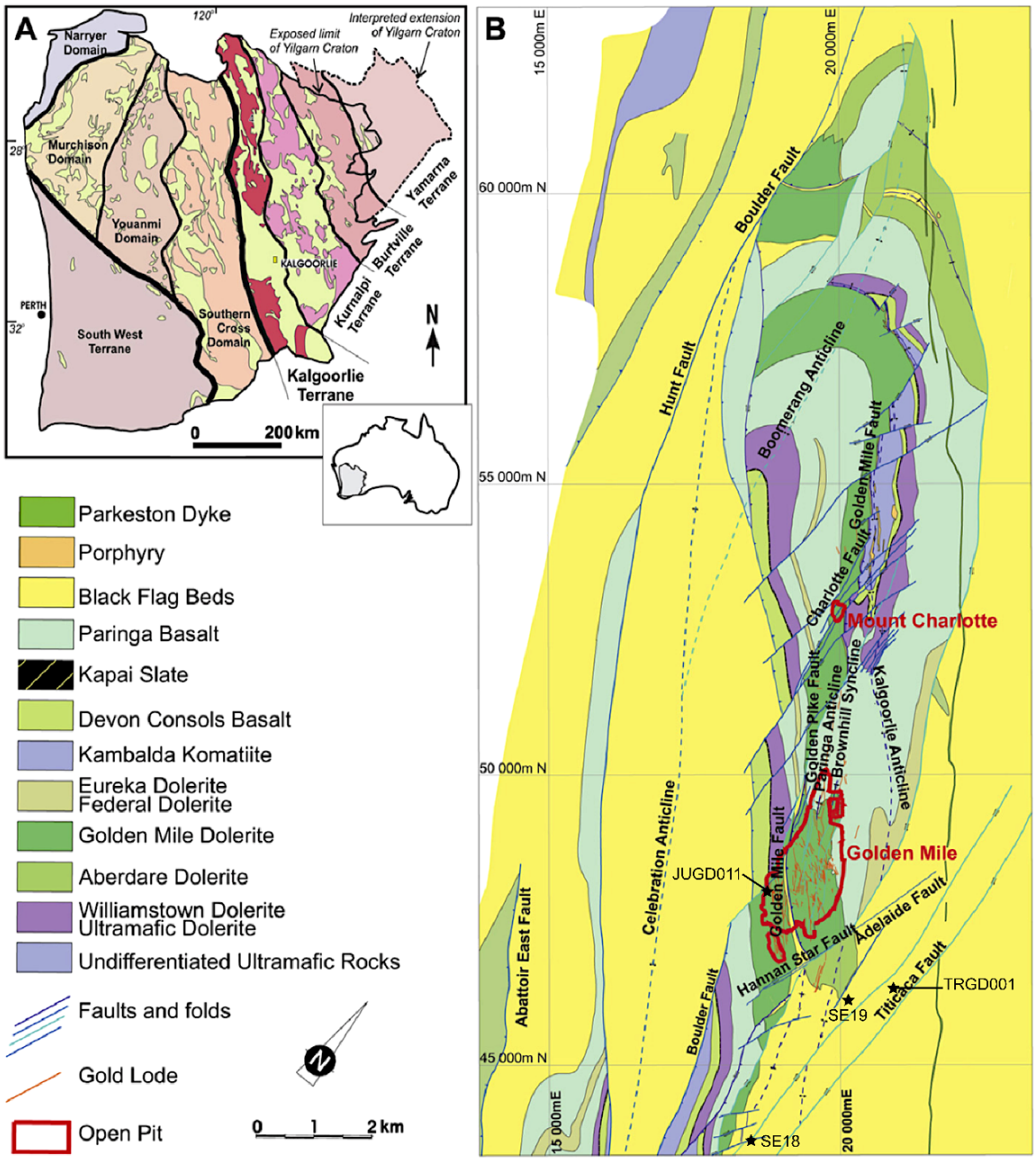

Figure 2.2 A geological map of the Kalgoorlie area showing approximate locations of surveyed drill holes. Modified from Vielreicher et al. (2016). Note this map uses the KCGM Oroya East grid reference.

2.4. Geological units of the Kalgoorlie Terrane:

2.4.1. Kambalda Sequence

2.4.1.1 Lunnon Basalt

Occurring beneath the Hannon's Lake serpentinite, the Lunnon Basalt and its regional equivalents (Scotia Basalt, centenary bore basalt ect) forms the substrate for the komatiite flows of the EGS (Squire et al., 1998, Hayman et al., 2015). The Lunnon Basalt Is interpreted to be a series of subaqueous meta-basaltic flows ranging in size from 5-20m thick and display a range of textures including pillowed and massive flows as well as well as basaltic breccias (Squire et al., 1998). A Re-Os isocron age for the Lunnon Basalt was established by Foster and Lambert (1996)at 2706 ± 36 Ma however due to stratigraphic constrains the approximate age for komatiitic volcanism was inferred to be closer to 2710 Ma (Squire et al., 1998)

2.4.1.2. Hannan's Lake Serpentinite

The basal unit of the Kalgoorlie stratigraphy, The Kambalda Komatiite and Hannan's Lake Serpentinite consists of a 300- 900m thick komatiitic unit (Bateman et al., 2001). These rocks show consists of a series several metre-thick flows of serpentinized ultramafic rocks with basal cumulates and spinifex textured tops(Bateman et al., 2001, Morris, 1993) REE and ND geochemistry conducted by Lesher and Arndt (1995) led them to suggests that the Hannan's Lake serpentinite has experienced as little as 2-5% crustal contamination. The formation of the Hannan's Lake serpentinite as well as a number of other komatiitic lava flow deposits across the Kalgoorlie Terrane to be linked to komatiitic volcanism occurring between 2710-2700Ma (Hayman et al., 2015, Kositcin et al., 2008)

2.4.1.3. Devon Consols Basalt

The Devon Consols Basalts previously the "Lower Hangingwall Basalts" sit stratigraphically above the Hannon's Lake serpentinite and are separated from the overlying pillowed and massive basalts of the Paringa Basalt by the Kapai Slate (Bateman et al., 2001, Vielreicher et al., 2016). Pillows and varioles can be seen regularly within the 60-100m thick high Mg basalts of the Devon Consols Basalt (Bateman et al., 2001). Geochemical data suggests that unlike the Hannan's Lake Serpentinite, the Devon Consols Basalt has experienced some assimilation of the surrounding continental crust (Said and Kerrich, 2010).

2.4.1.4. Kapai Slate (2692± 4Ma)

The Kapai slate acts as an important marker unit between the overlying Paringa Basalt and underlying Devon Consols Basalt in the Kalgoorlie-Kambalda area. Locally the Kapai Slate is a relatively thin <10m bedded volcanic siltstone which is thought to be the remains of a volcanic air-fall tuff, the distribution of this unit is widespread across the Kalgoorlie-Kambalda area, paired with the accurate grouping of zircon dates makes the Kapai Slate an excellent marker group. Zircon U-Pb dating was conducted by Claoué-Long et al. (1988) giving an age of 2692 ± 4Ma, an accurate date on the Kapai Slate is important as it will have implications and constraints for the formation times of the Paringa and Devon Consols basalts.

2.4.1.5. Paringa Basalt

The Paringa Basalt previously the "Upper Hangingwall Basalt" represents the uppermost basaltic unit of the Archean mafic to ultramafic Kambalda sequence (Bateman et al., 2001). Originally interpreted as a calc-schist the Paringa basalt was only recognised as a submarine flow with the discovery of pillows by Gustafson and Miller (1937). The Paringa Basalt ranges from fine to medium grained massive basalt and extensive pillow textures, sections of massive basalt are interpreted as subaqueous tabular or sheeted flows (Said and Kerrich, 2009). Gabbroic textures within the Paringa Basalt can be found and are thought by Said and Kerrich (2009) to represent slow cooling within the centre of thick flows.

2.4.1.6 Eureka Basalt

The Eureka basalt is an unofficial pillowed basaltic unit (described by Hugh Smithies GSWA unpublished data). This unit sits stratigraphically below the Golden Mile Dolerite and above the Paringa Basalt in the one drill hole it is encountered during this study (SE18). The Eureka basalt has been separated from the Paringa Basalt on the basis of geochemistry as it has distinct geochemical trends as well as falling within a separate thorium-basalt group as described by Barnes et al. (2012) (Fig 5.5).

2.5.2. Black Flag Group (Cycle One) (Kalgoorlie Sequence)

The Black Flag Group (BFG) or Kalgoorlie sequence, represents a series of thick, primarily felsic clastic and volcaniclastic rocks and local coherent volcanic rock units as well as dolerite bodies including the Golden Mile Dolerite. The samples of BFG observed in core during this project showed primarily angular dacitic breccias as well as volcanic sandstones, gritstones, and minor laminated mudstones. The Black Flag Group as described earlier has been subdivided into the early and late Black flag group by Squire et al. (2010). A Basal dacitic clast of the Black Flag group has been dated to give a possible maximum age of the BFG at 2686 ± 3Ma (Krapez et al., 2000). This is supported by the dating of the Kapai Slate in the underlying Kambalda sequence at 2692 ± 4Ma (Claoué-Long et al., 1988, Squire et al., 2010). The BFG is has been interpreted by Krapež and Hand (2008) to represent four cycles of tectonic uplift and subsidence starting in 2690Ma and ending in 2658Ma with each of these cycles lasting around 8Ma. These cycles are described by Krapež and Hand (2008) to operate in a four-stage system, 1) uplift and subaerial erosion 2) rapid subsidence leading to deep marine volcaniclastic sedimentation as well as rhyolitic, dacitic or minor basaltic volcanism 3) condensed section sedimentation and mafic magmatism which occurs at the point of peak subsidence 4) uplift and subsequent granite intrusion.

2.5.2.1. Golden Mile Dolerite (2680Ma ± 9Ma)

The Golden Mile Dolerite (GMD) is arguably the most economically important package of rocks within the Kalgoorlie Terrane as it is host to both the world famous Golden Mile gold deposit as well as the Mt Charlotte deposit, another significant greenstone gold deposit. This up to 750m thick dolerite unit described by Travis et al. (1971) as a dolerite sill which has undergone extreme differentiation into 10 distinguishable petrological-textural horizons or units. Units 1 and 10 are representative of the basal and upper chilled margins while units 2,3,4,5 and 9 are thought to represent in situ differentiation of an original magmatic pulse, while in contrast units 6-8 show evidence of at least three, later pulses of high iron magma (Travis et al., 1971) U–Pb age dating of zirconolite and xenotime conducted by Rasmussen et al. (2009) on the Golden Mile Dolerite in the Mt Charlotte area has given an age of deposition at 2680 ± 9Ma. This age coincidently puts the GMD within error of deposition of

the overlying Early Black Flag Group 2690-2680Ma (Kositcin et al., 2008). In the Kalgoorlie area, the Golden Mile Dolerite is found between the lower contact of the EBFG and the underlying Paringa Basalt. The contact between the Golden Mile Dolerite and the overlying EBFG is not extensively understood, which has inspired much of the controversy of the GMD. The interpretations range from the possible unconformable deposition of BFG sediments onto the GMD (Gustafson and Miller, 1937), pyroclastic breccias including GMD fragments (Golding, 1985), hydraulically brecciated contact aureole and erosional boundary (Krapež and Hand, 2008) to a carbonated series of basic flows interbedded with tuffs (Tomich, 1974).

2.5.2.2. Early Black Flag Group cycle one (2690Ma – 2680Ma)

The Early Black Flag Group (EBFG) consists of primarily feldspar-rich volcanic debris with minor volcanic quartz and plagioclase glomerocrysts (Squire et al., 2010). The presence of fragmented feldspar crystals suggests these rocks were deposited relatively quickly with minimal reworking. The beds of the EBFG consists of mostly massive graded and generally well-stratified beds, these beds largely lack mudstone and cross-bedded units. This evidence has been interpreted by Squire et al. (2010) to represent middle absent turbidites which have formed within a volcanic apron environment. Sections of the EBFG show monomictic felsic block and ash flow-like breccias within a matrix of felsic volcanic sandstone which suggests that at some point subaerial felsic volcanism has occurred (Squire et al., 2010).

2.5.2.3. Late Black Flag Group cycle one (2680Ma – 2665Ma)

The Late Black Flag Group (LBFG) conformably overlie the felsic sandstones of the EBFG, however, a marked change in both mineralogy and zircon age populations, suggest a change in regional conditions (Squire et al., 2010). The basal units of the LBFG have notably more volcanic quartz when compared to the underlying felsic beds of the EBFG. These quartz-rich beds are overlain or interbedded with coarse mafic conglomerates which can consist of up to 85% clasts of mafic and ultramafic material as well as granitic, dacitic and rare lithic clasts (Squire et al., 2010).

2.5.3. Merougil Group (Cycle two)

2.5.3.1 Early Merougil Group (2670Ma – 2660Ma)

Rocks of the Early Merougil Group are dominated by thick units of coarse-grained quartz-rich sandstones, in which the quartz is mostly volcanic in provenance. Volcanic sandstones of this unit have been found to have a unimodal distribution of zircon U-Pb ages dates (2670Ma – 2660Ma) as well as preserved juvenile volcanic fragments and an abundance of volcanic quartz crystals and crystal fragments (Squire et al., 2010, Krapez et al., 2000). This information has led Squire et al. (2010) to suggest that these successions are the result of a voluminous explosive eruption linked with the peak production of high Ca granites which was occurring at this time. The presence of trough cross-bedded and cross-stratified sandstones within the Merougil group suggest that reworking of the sediments before deposition had occurred in a fluvial-alluvial environment (Squire et al., 2010).

2.5.3.2. Late Merougil Group (2665Ma – 2658Ma)

Conglomerates and sandstones of primarily felsic volcanic material make up most of the rocks in the Late Merougil Group with the exception of minor occurrences of mafic and ultra-mafic clasts (Squire et al., 2010). Zircon ages taken from the late Merougil Group show a range of dates, the most interesting of which is a subgroup at 2665Ma which matches with the Early Merougil group. This data is interpreted by Squire et al. (2010) to represent the recycling of the Early Merougil Group in the formation of the Late Merougil Group in a similar way to the formation of the Later Black Flag Group.

2.5.4. Late basin sediments

2.5.4.1. Kurrawang Group (2658Ma – 2655Ma)

The Kurrawang Group represents the youngest succession of volcaniclastic rocks within the Kalgoorlie Terrane and includes both the Kurrawang Formation near Kalgoorlie and the Pottaroo turbidites near Granny Smith mine. Rocks of the Kurrawang formation are

dominated by felsic sandstones and polymictic conglomerates with an abundance of granitic, quartzite and up to 40% banded iron formation clasts (Krapež and Hand, 2008, Squire et al., 2010). Rocks of the Kurrawang Formation postdate the Archean volcanism of the Eastern Goldfields Superterrane and act as the final episode of deposition for the area (Squire et al., 2010). Detrital zircon ages for this group range from approximately 3500Ma to 2600Ma, this leads to the assumption that the rocks of the Kurrawang Group may be sourced through exhumation and reworking of the ancient crust. The source ancient crust is not known within the Kalgoorlie Terrane and may have been located in the Youanmi Terrane to the west (Squire et al., 2010).

2.6. Observed local geology of the Kalgoorlie-Kambalda area: The Kambalda Domain

A series of four co-funded drill holes provided by the Geological Survey of Western Australia within the South End region of Kalgoorlie offer a series of continuous stratigraphic columns, which are relied on heavily in this study. Drill hole SE18 offers the most complete stratigraphic column of the local geology intersecting six stratigraphic units from top to bottom; EBFG, GMD, Eureka Basalt, Kapi Slate, Paringa Basalt and the Hannon's Lake Serpentinite. The other drill holes JUGD011, TRGD001 and SE19 are all confined to the Golden Mile Dolerite and the surrounding EBFG rocks (Fig 6.1).

2.7. Structural history

The Yilgarn Craton has been extensively deformed and deformation styles have been used by many as an indicator of the tectonic setting (Swager, 1997, Mueller et al., 1988, Blewett et al., 2004). For this study, structural models and nomenclature will be adapted from Blewett et al. (2010).

2.7.1. Pre-D1 deformation

Evidence for pre-D1 deformation is not widely preserved within the EGS. Where it does exist, it is limited to small non-continuous packages of pre 2720Ma stratigraphy which occur on the boundaries of some large granite domes in the Kalgoorlie and Kurnalpi terranes.

These fabrics are not extensively understood due to the fractured and poorly constrained nature of these rocks (Blewett et al., 2010).

2.7.2. Deformation one (D1)

The first widely recognised major deformation event in the EGS was an ENE – WSW extensional event linked with significant crustal growth which likely occurred between 2720Ma and 2670Ma. This extensional event began with rifting of the eastern margin of the Youanmi Terrane around 2720Ma which coincides with the beginning of greenstone deposition in the EGS and is displayed through D1 fabric is displayed through recumbent folding events linked to intermittent compression (Blewett et al., 2010).

2.7.3. Deformation two (D2)

D2 occurs at the termination of the D1 extensional event and represents the beginning of the first large-scale ENE-WSW contractional or compressional event. The development of this event is speculated to developed as a diachroneity with the contraction beginning in the east followed by the west at 2670Ma and 2665Ma respectively (Blewett et al., 2004, Czarnota et al., 2010). This deformation is interoperated to be a relatively low strain event due to the lack of pervasive foliations instead manifesting itself in locally intense areas of upright NNW striking folds within the younger volcanic successions of the EGS (Blewett et al., 2010, Czarnota et al., 2010).

2.7.4. Deformation three (D3)

The D3 deformation represents the second round of ENE extension within the EGS. Like the D2 event D3 deformation occurred first in the east ~ 2665Ma, followed by the west ~2660Ma. This event is interpreted as a response to magmatic and tectonic thickening of the crust or possibly the result of tectonic plate slab rollback (Czarnota et al., 2010, Blewett et al., 2010). The development of granite cored domes and D3 extensional shear zones as well as the exhumation of both granites and greenstones are associated with the D3 events (Czarnota et al., 2010).

2.7.5. Deformation four (D4)

The D4 deformation event coincides with the primary gold depositing events within the EGS with only minor gold deposition occurring during D2 and D3. This span of tectonic activity has been subdivided into D4a) ENE -WSW contraction and D4b) NNW – SSE sinistral strike-slip shortening and thrusting (Blewett et al., 2010). ENE -WSW contraction during the D4a event led to the tightening of previous folds and the development of WSW thrusting along previously developed NNW trending faults. This folding overprints the fabric imposed during D3 late basin sequences. The D4b event is marked by the development of sinistral strike-slip shearing along previous NNW striking faults (Blewett et al., 2010). These evets are interpreted to have occurred between 2650 – 2655Ma (Blewett et al., 2010)

2.7.6. Deformation five (D5)

Locally intense dextral strike-slip faults and NE – SW shortening define the D5 deformation event, which developed across the whole of the EGS (Blewett et al., 2010). The timing of these events is interpreted to have occurred between 2650 - <2638±2Ma (Blewett et al., 2010).

2.7.7. Deformation six (D6)

D6 deformation makes up the last significant set of Archean deformation and was a low strain phase of vertical shortening and horizontal extension occurring <2630Ma (Blewett et al., 2010).

2.8. Intrusive events

The intrusive bodies of the EGS can be subdivided into two major groups high Ca and low Ca granites as well as three minor groups High Field Strength Element, Mafic and Syenitic (Champion and Sheraton, 1997).

2.8.1. High Ca granites

High Ca granites make up most of the granites of the EGS, including 60% of all granites and over 40% of all rocks in the EGS. These granites primarily consist of trondhjemite, sodic granodiorite, and granite, all of which are biotite bearing with 68 – 77% SiO_2 (Champion and Sheraton, 1997, Champion and Cassidy, 2007). The peak production of high Ca granites is thought to have occurred between 2720Ma – 2660Ma. Champion and Cassidy (2007) have suggested that these high Ca granites are the result of high-pressure melting of basaltic protoliths either through the melting of subducted oceanic crust or within the thickened mafic crust.

2.8.2. Low Ca granites

Although not as prevalent as their high Ca counterparts, the low Ca granites of the EGS make up around 20% of the total granites in the area (Cassidy et al., 2004). The low and high Ca granites can be hard to distinguish, however, the low Ca granites tend to be more abundant in alkali feldspars resulting in monzogranites and syenogranites (Champion and Sheraton, 1997). These granites are chemically distinct from their high Ca counterparts with high LILE (large-ion lithophile elements) and enriched in LREE (Light Rare Earth Elements). The low Ca granites formed much later than the other subgroups of granite at <2665Ma, therefore, occurring too late to be a significant source for the Archean sedimentary units of the EGS (Squire et al., 2010). Champion and Cassidy (2007) interpret the low Ca granites to be the product of partial melting of a tonalitic composition source, probably as a result of the reworking of the older high Ca felsic crust.

2.8.3. HFSE granites

The High Field Strength Element (HFSE) granites occurred in much lower volumes then the high and low Ca granites and tend to display A-type characteristics with high silica (>74% SiO_2) (Champion and Cassidy, 2007). The emplacement of these granites is rare in the EGST and range from approximately 2685Ma – 2660Ma (Champion and Cassidy, 2007, Squire et al., 2010).

2.8.4. Mafic intrusions

The mafic granites of the EGS are a chemically diverse group of rocks which includes hornblende-pyroxene diorite, hornblende-biotite tonalite, trondhjemite, biotite-hornblende granodiorite and biotite granite with a range of SiO_2 values (<60- >70% SiO_2) (Champion and Sheraton, 1997, Champion and Cassidy, 2007). Rocks of this group are thought to have been emplaced between 2690Ma and 2650Ma; these granites can be seen to intrude the packages of the Kalgoorlie and Kambalda Sequences (Squire et al., 2010, Champion and Cassidy, 2007).

2.8.5. Syenite intrusions

Granitoids of a syenitic composition are rare within the EGS and similar to the low Ca Granites were emplaced later than the other subgroups (<2650-2640Ma) (Champion and Cassidy, 2007). These syenites range in composition from hornblende-clinopyroxene syenite to quartz syenites and constitute a relatively low volume intrusions with distribution generally confined to lineaments (Champion and Sheraton, 1997).

2.8.6. Dolerite intrusions

Mafic intrusions of thick internally differentiated dolerite sills occur in both the Kambalda and Kalgoorlie sequences and can be divided into two separate chemically distinct units (Squire et al., 2010). The first group of doleritic units are stratigraphically constrained to intrude the upper Kambalda sequences, and include the Defiance Dolerite at St Ives, Williamstown Dolerite, Enterprise Dolerite and Mount Pleasant Sill around Kalgoorlie. Many of these intrusions share a very similar immobile element geochemistry and spatial distribution with the basaltic lavas of the Paringa Basalt (Squire et al., 2010). An age date for the Williamstown Dolerite at 2696 ± 5Ma suggests that these intrusions are likely a result of the last stages of greenstone emplacement (2715-2620Ma) (Czarnota et al., 2010, Fletcher et al., 2001).

The dolerites of group two although texturally similar to the type one dolerites, can be differentiated through the recognition of a more primitive immobile element geochemistry (Squire et al., 2010). These units include the Golden Mile Dolerite, Condenser Dolerite and the Ora Banda Sill, which all intrude exclusively the beds of the Black Flag Group (Squire et al., 2010). These units are interpreted to have formed later than the group one dolerites with the GMD forming at 2680 ± 9Ma (Rasmussen et al., 2009, Squire et al., 2010).

3.0. Methods

3.1. Core logging

The fieldwork segment of this project consisted of the graphic logging and sampling of four recent Co-funded stratigraphic drill holes (SE18/W1, SE19/W1, TRGD1/A and JUGD0011) available through the Geological Survey of Western Australia and KCGM at the GSWA Joe Lord Core Library in Kalgoorlie WA. These drill holes extend over a significant part of the strike length of the Golden Mile Dolerite giving a new insight into the internal architecture and emplacement processes of the GMD. While logging these drill holes special attention was given to the internal textural variations within the Golden Mile Dolerite. Where visible the contact relationships between the GMD and surrounding units were studied in greater detail so as to determine the likely mode of emplacement of the GMD. The systematic graphic logging of these holes was done at 1:1000 scale where 1cm = 10m with greater detail given to areas of interest. Samples of Golden Mile Dolerite and the overlying volcaniclastic rocks of the Black Flag Group were taken as reference samples, some of which were also processed into thin sections and for geochemical analyses for further investigation.

3.2. Geochemistry

Systematic sampling of drill hole JUGD011 was conducted at 50m intervals downhole as well as additional samples taken wherever an obvious change in lithology or texture could be seen. A total of 25 geochemical samples were taken from JUGD011, and these samples were processed for whole rock geochemistry at the GSWA Lab in Perth WA by means of several analytical methods. An additional 20 whole rock geochemical analyses of the GMD in JUG011 were supplied for this project by (P. Hayman, R. Cas and R. Squire unpublished data). additional whole-rock geochemical data were supplied by Hugh Smithies of the GSWA, this data included geochemistry for a further eight drill holes including DDHSE18 and its wedge SE18W1 which is a primary hole which was graphically logged. This data was produced at the GSWA geochemical facilities and was combined with four geochemical samples of SE18 and SE18W1 collected while logging to give better geochemical coverage within the holes. All geochemical data was compiled, as to compare geochemical trends between drillholes, unfortunately no samples were analysed by both laboratories to determine possible differences due to method change. However, the collected data is

generally consistent across laboratories where samples are adjacent. The geochemistry conducted in this study focuses primarily on the variations within the Golden Mile Dolerite. Work conducted by Travis et al. (1971) suggested a ten unit subdivision of the GMD, and the geochemical data obtained in this study will be compared to their findings.

3.2.1. Geological Survey of Western Australia methods (provided by Hugh Smithies of the GSWA)

All samples were analysed by BV (Bureau Veritas) Minerals, in Canning Vale, Perth, Western Australia. Samples were visually inspected and any weathering or vein material was removed. Each sample was crushed in a plate jaw crusher and milled in a low-Cr steel mill to produce a pulp with a nominal particle size of 90% < 75 μm. A representative pulp aliquot was analysed for 13 elements as major components, loss on ignition, and 54 elements as trace elements (ppm or ppb). Major elements were determined by x-ray fluorescence (XRF) spectrometry on a fused glass disc. A fragment of each disc was then laser-ablated and analysed by ICP-MS for 51 of the 54 minor elements. Gold, Pd and Pt were analysed on a separate pulp aliquot by lead-collection fire assay and ICP-MS. Data quality was monitored by 'blind' insertion of sample duplicates (i.e. a second pulp aliquot), GSWA internal reference materials, and the certified reference material OREAS 24b (www.ore.com.au). BV Minerals also included duplicate samples (including OREAS 24b), variably certified reference materials, and blanks. An assessment of accuracy and precision was made using data for 17 analyses of OREAS 24b, determined during the analysis of greenstones. For analytes where the concentration is at least ten times the lower level of detection, a measure of accuracy is provided by the agreement between the average determined value and the certified value which is < 0.05 for all analytes apart from Be and Cu. In terms of precision, the percent relative standard deviation (RSD%) or covariance for analysis of OREAS 24b is < 10% for all analytes apart from As, Cu, Ni, Sc and Zn. Similar levels of agreement were found for parent-duplicate pairs. All blank values were less than three times the lower level of detection

3.2.1 University of Tasmania methods. (provide by the University of Tasmainia)

SUMMARY OF XRF ANALYSIS (X-Ray Fluorescence Analysis)

School of Earth Sciences - CODES, University of Tasmania Phil.Robinson 11/11/09

Instrument PANalytical Axios Advanced X-Ray Spectrometer

X-Ray Tubes: 4kW max. Rh anode end window.

Elements analysed: F, Na, Mg, Al, Si, P, S, K, Ca, Ti, Mn, Fe and trace elements Sc, V, Cr, Co, Ni, Cu, Zn, Ga, Ge, As, Se, Br, Rb, Sr, Y, Zr, Nb, Mo, Ag, Cd, Sn, Sb, Te, I, Ba, La, Ce, Nd, W, Tl, Pb, Bi, Th and U.

3kW max. Au anode end window.

Elements analysed: extra sensitivity for Sc, Ba, La, Ce, Nd, Sb, Sn, Ag, Cd, Te.

Crystals: PX-10, LiF 220, PX-1 (for F, Na and Mg), curved PE002, curved Ge111

Collimators: Coarse (0.7mm), fine (0.3mm) and high resolution (0.15mm)\

Detectors: Gas flow proportional counter with P10 gas (10% methane in

argon), sealed Xe Duplex and Scintillation Counter.

Sample Changer: PANalytical X-Y sample changer with capacity for 96 fusion discs and 64 pills.

Sample Preparation

Major Elements: 32mm fusion discs prepared at 1100 degrees C in 5%Au/95%Pt crucibles

0.500g sample, 4.500g 12-22 Flux (Lithium Tetraborate-Metaborate mix), 0.0606g LiNO3 for silicates. Platinum/5% gold moulds used for cooling.

Sulphide bearing samples have a different mix with more $LiNO_3$ as oxidising agent and the mix is pre-ignited at 700 degrees C for 10 minutes. Ore samples and ironstones use 12/22 flux and a higher flux/sample ratio. Dolomites and limestones need pure lithium tetraborate as a flux. Iodine vapour is used as a releasing agent to remove discs from the mould.

Trace Elements: 32mm diameter pressed powder pills (10g, 3.5 tonnes/cm^{-2}), Sample Binder PVP-MC.

Corrections

Corrections for mass absorption are calculated using PANalytical Super-Q software with its Classic calibration model and alpha coefficients. In house inter-element corrections are also applied. PANalytical ProTrace and Compton scattering can also be used for many trace elements.

Calibration

Pure element oxide mixes in pure silica, along with International and Tasmanian reference rocks are used. Numerous checks of reference rocks and pure silica blanks are run with each program.

References

Robinson P. 2003. XRF analysis of flux-fused discs. Geoanalysis 2003, The 5th International Conference on the Analysis of Geological and Environmental Materials, Abstracts, p90.

Watson J.S. 1996. Fast, Simple Method of Powder Pellet Preparation for X-Ray Fluorescence Analysis. X-Ray Spectrometry, 25, 173-174.

3.3. Microscopy

From the samples collected during logging 27 samples were selected for preparation of polished thin sections. These samples were selected for several reasons including:

1) to assess the variation in mineralogy and texture within the Golden Mile Dolerite
2) to compare the basaltic sections of the GMD with select basaltic apophyses in conjunction with geochemical data
3) to observe the contact relationships between basalt and sedimentary units on the microscale
4) to investigate possible affinities of mafic clasts in the overlying andesitic-dacitic breccias of the Black Flag Group

Each thin section was studied under transmitted and cross polarised light microscopy, in conjunction with reflected light when necessary to identify opaques.

4.0. Lithofacies of the Kalgoorlie area

Thick sequences of submarine and subaerial clastic and volcaniclastic rocks of the Black Flag Group overlie several thick mafic and ultramafic units of the Kalgoorlie sequence in the Kalgoorlie region of Western Australia (Fig. 4.1). The observed lithofacies units of the Black Flag Group show significant differences in clast composition, chemistry and texture to rocks of the Kalgoorlie sequence, which reflects the different events responsible for each succession (Squire et al., 2010) However, the lithofacies of the Golden Mile Dolerite also show a range of internal textural and chemical variations (basalt, dolerite, gabbro to granophyre), which will be described here, beginning with the Black Flag Group.

4.1. Clastic facies of the Black Flag Group

4.1.1. Black mudstones

Description. Beds of black mudstone between >1m and up to 30m thick are common throughout many of the holes observed. These units are of importance as they reflect the ambient environment conditions at the time of deposition. They often occur at the boundaries of the Golden Mile Dolerite and its apophyses, showing clear contact relationships. Carbonate veining is common within the black mudstones beds and competency of these units is often low with most of the core fractured along a common cleavage. Pyrite is common within some mudstone horizons both as fine disseminated, veined and euhedral pyrite. Contacts with other sedimentary units and the Black mudstones are often sharp or undulating lacking a gradational change (Fig. 4.1). No samples of mudstone were collected for geochemical or thin section sampling.

Interpretation. The relative thickness (up to 30m) and homogeneity of the black mudstones suggest that these formed in a low energy, anoxic deep basin system through pelagic sedimentation (Henrich and Hüneke, 2011, Hüneke and Henrich, 2011). Non-graded to sharp top and bottom contacts between the mudstones and the surrounding volcaniclastic units rules out the possibility of a turbidity flow origin. Instead, these units likely represent long spans of time between the volcanic eruptions responsible for the production of the andesitic-dacitic breccias and gritstones discussed below.

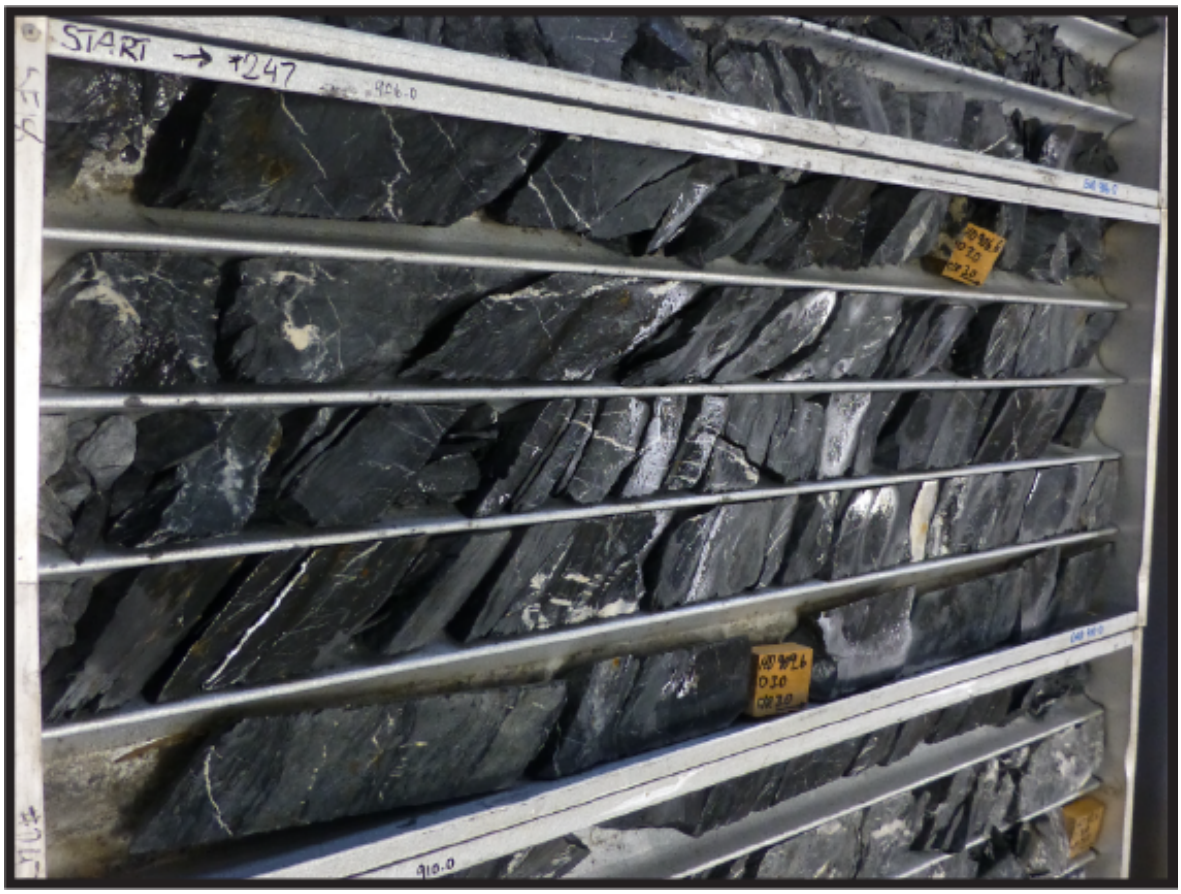

Figure 4.1. DDHSE18 A thick black mudstone unit commonly associated with carbonate veining and extensive pervasive carbonate alteration (DDHSE18, 247m).

4.1.2. Matrix-supported monomictic, feldspar phyric angular breccias

Description. The uppermost unit observed in DHH - SE18 of the Black Flag Group consists of >200m of variably altered high SiO_2 andesitic-dacitic breccias. These breccias are generally massive and ungraded with beds ranging in thickness from 10-200m and are generally separated from successive beds by sharp contacts with the graded polymictic volcanic sandstone beds and gradational contacts with the pebbly gritstone facies. This unit consists of poorly sorted matrix-supported angular to sub-rounded, feldspar phyric clasts. Clasts of this breccia range in size from sand-sized particles (>1cm) through to boulder-sized blocks (>256mm) with some mega clasts (>2m). The matrix and clasts of this facies share strikingly similar compositions and when observed in thin section, the matrix seems to solely consist of broken plagioclase crystal fragments and disintegrated clasts. Within the breccias,

the clasts seem to be randomly orientated lacking any major indication of flow direction. The mineralogy of these clasts, as observed in thin section 222903 consists of a fine-grained altered groundmass with phenocrysts of plagioclase feldspar 1mm- 2mm and relic hornblende crystals. Andesitic-dacitic breccias of a similar composition and clast shape to those seen in SE18 occur in TRGD001/A (150m-190m, 250m-260m). These breccias differ from those in SE18 with a matrix of medium sandstone (Fig. 4.2 B) and occur in much thinner beds. Small horizons of (<50cm) black heavily altered clasts occur throughout the andesitic-dacitic breccias of SE18. These clasts when observed in thin section are mineralogically similar to the andesitic-dacitic breccias consisting primarily of broken plagioclase crystals within a heavily chlorite altered matrix (Fig. 4.2C, D).

Interpretation. The clasts of these breccias are suspended within a matrix of the same composition as the clasts, this may represent the disintegration of clasts to form a matrix. a possible explanation for the formation of these homogenous. Monomictic angular breccias is through dome collapse as described in Ui et al. (1999) with the formation of a block and ash flow breccias. For this method of formation to be true then andesitic-dacitic subaerial or subaqueous lava dome forming volcanism must have occurred during the formation of this lithofacies (Calder et al., 2015). This observation has been made previously by Squire et al. (2010) who described a felsic monomictic cobble conglomerate intercalated with feldspar-rich sandstone which they linked with a subaerial source. The sub-rounded morphology of some of the andesitic-dacitic clasts suggests that this unit has undergone a degree of reworking and although they resemble primary block and ash flow breccias these units may represent resedimented block and ash flow material. The andesitic breccias of TRGD001 seem to represent correlatable units to those seen in SE18, the matrix is texturally different to those seen in SE18 but may just be finer grained andesitic-dacitic material. As there is no evidence of a hot in situ emplacement for these breccias the name Andesitic-dacitic-mass flow breccia will be preferred to block and ash flow.

4.1.3. Feldspar rich pebbly gritstones

Description. Beneath the monomictic andesitic breccias of the Black Flag Group seen in DDHSE18, a change in lithofacies to a pebbly gritstone facies, occurs between approximately 525m and 1340m in the drill hole. The predominant texture seen within this

lithofacies are massive beds (5-50m thick) of poorly sorted crystal-rich pebbly volcanic gritstone. These beds are compositionally very similar to the monomictic andesitic-dacitic breccias described above however they lack the large clast component. containing primarily 2-5mm crystals of plagioclase feldspar as well as minor lithic sandstone and mudstone intraclasts (Fig. 4.2C). Heavy chlorite alteration throughout the pebbly gritstone in DDHSE18 tends to obscure texture. Medium-grained grey sandstones (2-4mm) up to 50m thick and black mudstones as described above occur through the packages. No samples of these units were collected for geochemical or thin section sampling. The intersections between the underlying mudstone units show possible mixing with the gritstones (Fig. 4.2E)

Interpretation. These coarse crystal-rich gritstones are likely the result of felsic volcanism possibly sharing a similar source as the andesitic-dacitic mass flow breccias described above. The mixing at the bottom contacts between the black mudstone and volcanic gritstone units suggest that these gritstones were emplaced onto a wet unconsolidated sediment pile (Fig. 4.2E) (Mills, 1983, Leeder, 2009). The incorporation of angular mudstone rip-up clasts within the thicker beds (Fig. 4.2C) suggests these beds were emplaced under higher energy conditions as to dislodge underlying intraclast fragments of mudstone. For these mudstone clasts to be incorporated as angular fragments the source mudstone must have been solidified in contrast to the soft sediment deformation seen at the contacts (Mills, 1983, Leeder, 2009). This suggests that these units which are interpreted to be higher energy resedimented units were emplaced onto a low energy pelagic paleoenvironment discussed for the mudstone units above (Leeder, 2009, Henrich and Hüneke, 2011, Hüneke and Henrich, 2011). This change in depositional environment may be accounted for by resedimentation possibly down a basin slope into a deep subaqueous environment (Meiburg and Kneller, 2010). These units are comprised of essentially the same material as the as the andesitic-dacitic mass flow breccias described above with the exception of the mudstone rip-up clasts. The feldspar rich pebbly gritstone units may represent a finer grained equivalent of these resedimented mass flow deposits.

Figure 4.2. A) Common andesitic-dacitic mass flow breccias of the Black Flag Group (SE18 199m, sample 222903). B) Angular andesitic breccia similar to those seen in SE18 however in a more sandstone rich matrix (TRGD001, 171m) C) possible chlorite altered andesitic-dacitic clast within the Black Flag Group (SE18, 289m, sample 222593) D) rounded polymictic conglomerate containing possible chlorite altered andesitic-dacitic clast (TRGD001, 277m). E) Coarse feldspar crystal-rich volcanic gritstone with intra-clasts of black mudstone (SE18,619m) F) Massive coarse feldspar crystal-rich volcanic gritstone (TRGD001, 147m).

4.1.4. Graded and cross-bedded volcanic sandstone beds.

Description. Several matrix-supported, polymictic, moderately bedded and graded beds which are generally <2m thick and occur within the andesitic-dacitic breccias (SE18 215m-275m) (Fig. 4.2A, B). Clasts within these beds are rounded to subangular to subrounded with sizes ranging from poorly sorted, coarse pebbly conglomerates at the bottom (32-64mm) fining upward to laminated clay/silt beds at the top. The tops of these beds often show signs of cross-lamination (Fig. 2A). Clasts in these beds include altered andesite, crystal fragments of quartz and feldspar, clasts of laminated mudstone and volcanic sandstone clasts. An extensive body of graded polymictic sedimentary beds occurs in TRGD001 (410-760m). These beds range in clast size from coarse gritstone (4mm) to mudstone beds. The mudstone beds of this unit display flame structures (Fig. 4.3 D) at the contact between mudstone and sandstone beds. The flame structures indicate the younging direction and show at least 3 bedding reversals.

Interpretation. The bedded sedimentary horizon of SE18 may represent a break in volcanic activity in which erosion and related fluid supported transport processes resumed leading to the sorting and rounding of clasts seen in these beds. The polymictic nature of these beds may suggest that the material forming these rocks was able to draw from a range of sources possibly through fluvial transport. The large polymictic beds seen in TRGD001 likely represent a series of turbidite flows (Meiburg and Kneller, 2010, Leeder, 2009). Turbidity current related flows would suggest a subaqueous environment associated with the mass movement of sediment down basin or continental edge slopes into deeper water environments possibly associated with subaqueous channels (Meiburg and Kneller, 2010, Schulten et al., 2018, Lowe, 1982). These turbidites may correlate with the series of well-graded polymictic beds seen in SE18 as a distal relationship (Fig. 4.3 A B). The bedding reversal seen in the flame structures of this unit suggests a series of folds which are not uncommon to these sequences, and likely are due to one of the many deformation events (Blewett et al., 2010, Czarnota et al., 2010, Mills, 1983).

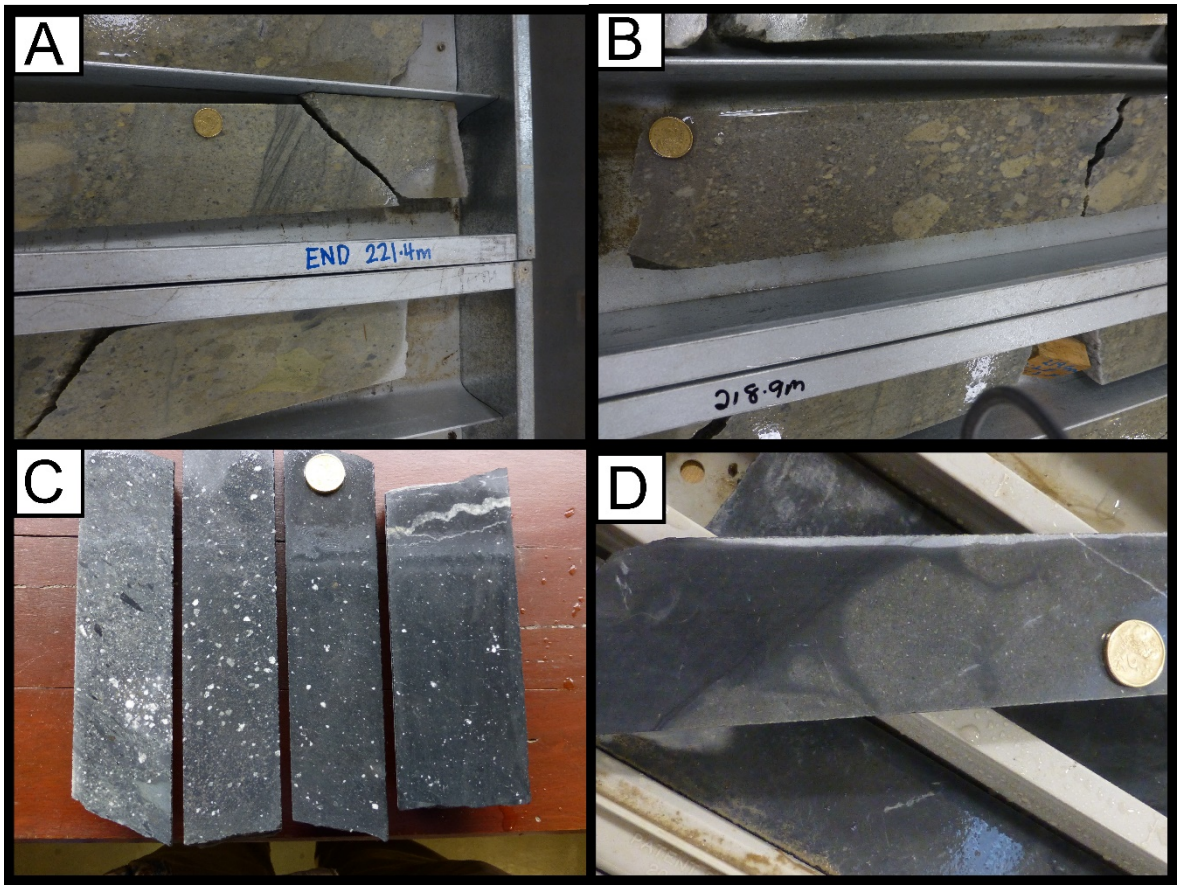

Figure 4.3. Samples showing variation within the volcanic gritstone facies. A) Cross-bedded siltstone top of a graded bed (SE18 221m) B) polymictic bedded pebbly conglomerate through to medium sandstone, note the younging direction is to the Left (SE18, 218m). C) Crystal rich volcanic gritstone showing the effect of chlorite alteration with the destruction of texture from least altered (left) to most altered (right) (SE18, 900m-950m). D) Mudstone flame structures showing younging direction within bedded turbidite sequences (TRGD001, 700m).

4.2. The Golden Mile Dolerite

The Golden Mile Dolerite was intersected in each of the major drill holes studied and is the focus of this project and shows significant internal variations, which will be discussed in detail. The older drill hole JUGD011 intersects the most complete section of the Golden Mile Dolerite consisting of a single continuous intersection of dolerite with an observed thickness of approximately 960m in core. In contrast, more recently drilled holes indicate that it can consist of multiple mafic units that are separated by black mudstone horizons, for example drill holes SE18 and TRGD001 show multiple dolerite bodies separated by black mudstone beds. The Aberdare Dolerite (intersected in SE19 and TRGD001) is interpreted by (O'Connor-Parsons and Stanley, 2007, Bateman et al., 2001) to be a thinner 600-700m thick chemically equivalent dolerite sill which shares the same stratigraphic position as the Golden

Mile Dolerite. For this study, the GMD and Aberdare Dolerite will be considered as equivalent units and observations will be made accordingly. The GMD consists of a range of internal textural and compositional petrological facies, which will be described below.

4.2.1. Coherent basalt

Description. Fine-grained to aphyric coherent basalt is common within the Golden Mile Dolerite and was observed in all of the studied drill holes (e.g. SE18/W1, 1345m-1411m, 1690m-1780m, 1875m-1892. TRGD001/A, 1335m-1405m). Scattered thin basaltic units (<1m-2m) occur in the sedimentary units above and below the main GMD units (SE19/W1, 155m-335m, 2447m-2570m. JUGD011 220m-490m, 645m-680m, 1090m-1176m. SE18, 1460m-1530m). The coherent basalts of the Golden Mile Dolerite occur either as part of a larger body which coarsens gradationally towards the centre from top and bottom or as multiple thin <1m to approximately 10m thick basaltic units which occur in the surrounding sediments above and below the major dolerite bodies. The primary mineralogy of these basaltic units consists of mostly sub equal proportions of plagioclase feldspar (now clinozoisite) and clinopyroxene (now chlorite) within a large portion of heavily altered fine grained crystaline groundmass. Skeletal leucoxene after ilmenite alteration as well as chlorite/carbonate/epidote alteration is common within the fine-grained basaltic sections of the larger dolerite bodies such as in JUGD00l (220m-490m) (Bateman et al., 2001). The contacts between coherent basalt and mudstone show cross cutting to interfingering sharp to irregular relationships with the surrounding sedimentary units of the BFG (Fig. 4.4)

Interpretation. The fine-grained basaltic sections of the major dolerite bodies likely represent parts of basalt lava flows or the faster cooling margins of intrusive bodies (Marsh, 2015, McPhie et al., 1993, Harris and Rowland, 2015). The thin units of fine basalt intercalated in mudstone above and below the thick units of basalt-dolerite of the GMD could represent thin lava flows or represent offshoots of a mixture of small dykes and sills which branched from the main body during intrusive emplacement (Marsh, 2015). These then cooled rapidly due to their inherent low surface area to volume ratio and low capacity to retain heat (Harris and Rowland, 2015). Basalt lava flows are however, rarely less than 1m thick, and almost never only cms or mms thick as found marginal to the main units of the GMD in some holes (Harris and Rowland, 2015, McPhie et al., 1993).

4.2.2. Mudstone matrix-supported, mixed basalt-mudstone breccia

Description. Breccias of wispy to blocky fragments of basalt within a matrix of black mudstone occur associated with the boundary zones of the coherent basalts and are often gradational into them. these Breccias of this description occurred in all the observed holes, primarily where direct contact between coherent basalt and black mudstone occurred (SE18+W1 1460m, 1525.7m, 1500m-1690m; JUGD011 1185m-1190m, 1230m, 1253m). Clast abundance in these breccias tend to diminish with distance from the contact zone and the highest abundances occur several centimetres from this zone, where jigsaw fit and rotated clast textures are common (Fig. 4.4). The larger basaltic clasts of these breccias as seen in (Fig. 4.4) sometimes show internal fractures which fill with the surrounding mudstone (SE18W1, 1580m-1690m). These clasts range in size from <1cm to ~5cm and the bedding of the black mudstone that forms the matrix is disturbed and destroyed where they occur (Fig. 4.4). The basaltic clasts of these breccias do not show alignment or mechanical rounding, however, some of these contacts show globular clasts of basalt which do not always fully detach from the associated basaltic body. Not all contacts between the Golden Mile Dolerite and the Black Flag Group show these fragmental textures with irregular, undulating and inter-fingering contacts common (Fig 4.4)

Interpretation. The mudstone matrix supported basalt-mudstone breccias of the Golden Mile Dolerite could be sedimentary debris flows or quench-fragmented peperitic margins of lava flows (base) or top and bottom of shallow intrusive sills. Features that would distinguish these alternatives are the position of these breccias in relation to the dolerite bodies (McPhie et al., 1993) The basaltic breccias that are observed occur on both the top and bottom contacts of the Golden Mile Dolerite, this rules out the possibility of a basal peperitic contact of lava flow as well as a debris flow (McPhie et al., 1993, Busby-Spera and White, 1987). This may represent the burrowing of a basaltic lava flow but due to the extent of the GMD and the lack of other lava flow indicators this is unlikely. This leaves the interpretation that these breccias are the peperitic top and bottom contacts of a syn-intrusive dolerite body (White et al., 2000, Busby-Spera and White, 1987, McPhie et al., 1993, Harris and Rowland, 2015). These breccias are then interperited as the peperitic top and bottom margins of the sill as intruded through the unconsolidated and water saturated mudstones of the Black Flag Group (Van Otterloo et al., 2015a, Busby-Spera and White, 1987). This was likely beneath a subaqueous

deep basin environment represented by the pelagic/anoxic black mudstones, and the association with the subaqueous association of the overlying Early Black Flack Group sediments (Squire et al., 2010, Henrich and Hüneke, 2011, Hüneke and Henrich, 2011). The fragmentation of the basalt and the subsequent loss of coherency in the bedding of the mudstone units suggests the fluidisation and mobilisation of the sediments into the interstitial space occurred as the sill intruded the wet unconsolidated sediment (Kokelaar, 1982, White et al., 2000, McPhie et al., 1993) . The larger angular clasts (Fig. 4.4) may represent rapid, brittle quench fragmentation reactions between the water-saturated sediments and the hot magma interface due to their internal fracturing and blocky morphology. In contrast, the more globular clasts may represent dynamic mixing of fluidal basalt and water-saturated sediment (Busby-Spera and White, 1987, Kokelaar, 1982)

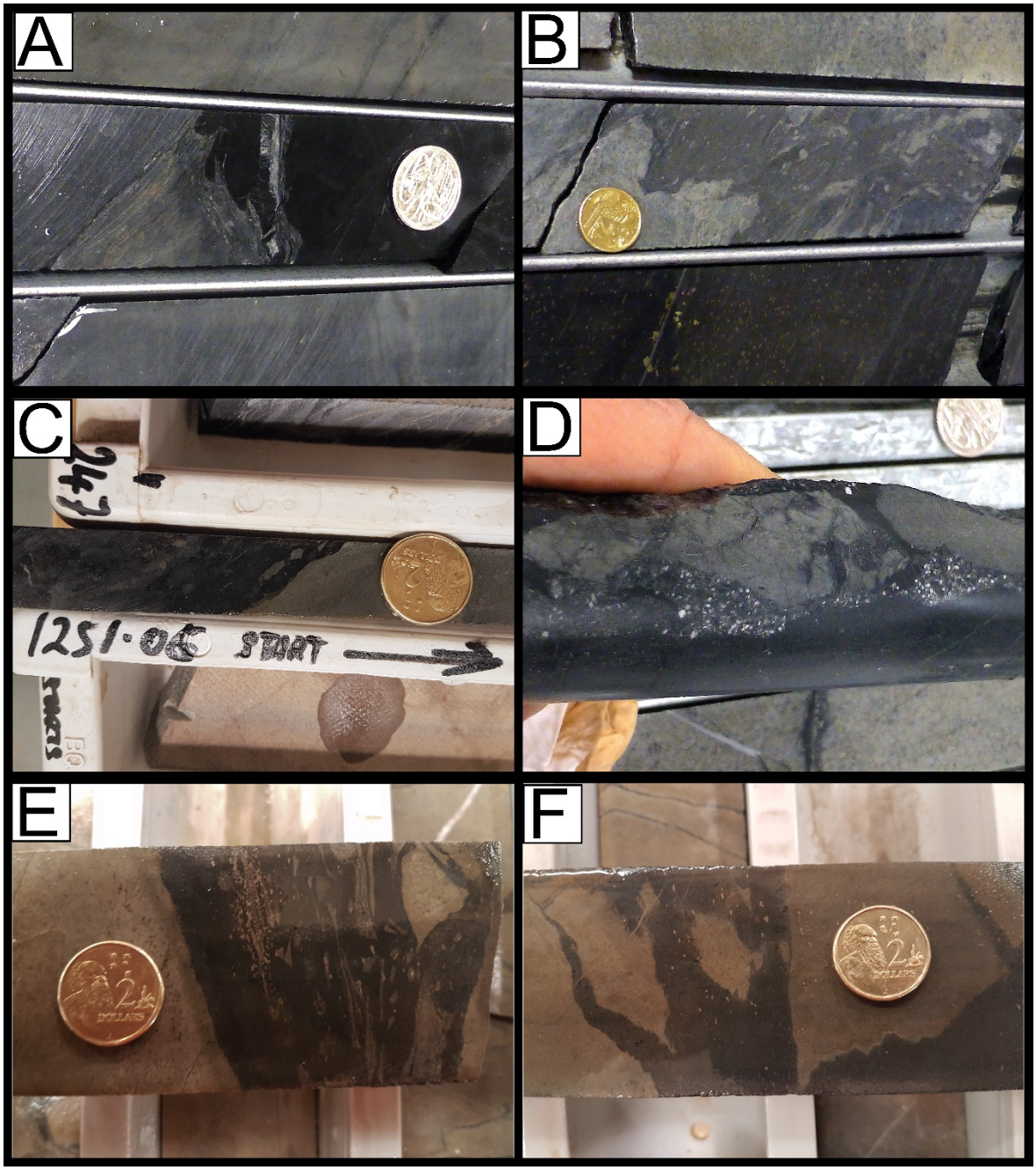

Figure 4.4 A) intrusive wispy contact between a basaltic apophysis and the surrounding black mudstone unit (SE18W1, 1477m) B) Peperitic contact at the base of a Golden Mile Dolerite body, Note the extensive distraction of bedding and wispy fragments of basalt distributed throughout the surrounding mudstones (SE18, 1460m). C) A peperitic margin between an apophysis of the Golden Mile dolerite and the overlying Black Flag Group mudstones. D) Fragments of the Golden Mile Dolerite which show possible contraction fractures and infill of black mudstone in an assumed peperitic contact (SE18W1 1607m). E) Peperitic margin between a basaltic unit and thin mudstone bed showing chilled a margin on the main basalt body (TRGD, 1341m) F) peperitic angular basaltic breccia within a black mudstone matrix showing jigsaw fit textures (TRGD001, 1340m).

4.2.3. Coherent dolerite

Description. The lower sections of the main body of the Golden Mile Dolerite consists of a variably altered 1-2 mm equigranular dolerite (JUGD011 490m- 600m, SE18 1830m-1870m, TGRD001/A 195m-245m,1405m-1500m, 1510m-1560m, 1630-1645m, 1770m-1815m). These dolerites are gradational with the coherent basalt facies, and in turn transitions into gabbro (see below) in the centre of thicker bodies (e.g. JUGD011, TRGD001). The mineralogy of these dolerites consists of primarily subequal proportions of relic plagioclase feldspar and pyroxene with minor Fe-oxides such as limonite, magnetite and leucoxene (1% opaque, 54% pyroxene 45% plagioclase, Sample 222908). The large relic plagioclase crystals are seen in these dolerites (samples 222908, 222907) show sub-ophitic textures, overgrowing smaller relic pyroxenes (Fig.4.5 A, B).

Interpretation. The medium grained dolerites of the Golden Mile Dolerite are interpreted to be the result from slow cooling and crystallisation in the interior of GMD units, away from the more rapidly cooled basalt margins (Marsh, 2015). Dolerite represents the continuation of fractional crystallization of the coherent basalt facies. This is supported by the gradational contacts with both the finer aphyric basalt and coarser gabbroic sections of the GMD. The increasing grain sizes from marginal basalt to dolerite and subsequently gabbro is suggestive of the differentiation which would be expected from a mafic intrusion (McDougall, 1964, O'Connor-Parsons and Stanley, 2007, Marsh, 2015).

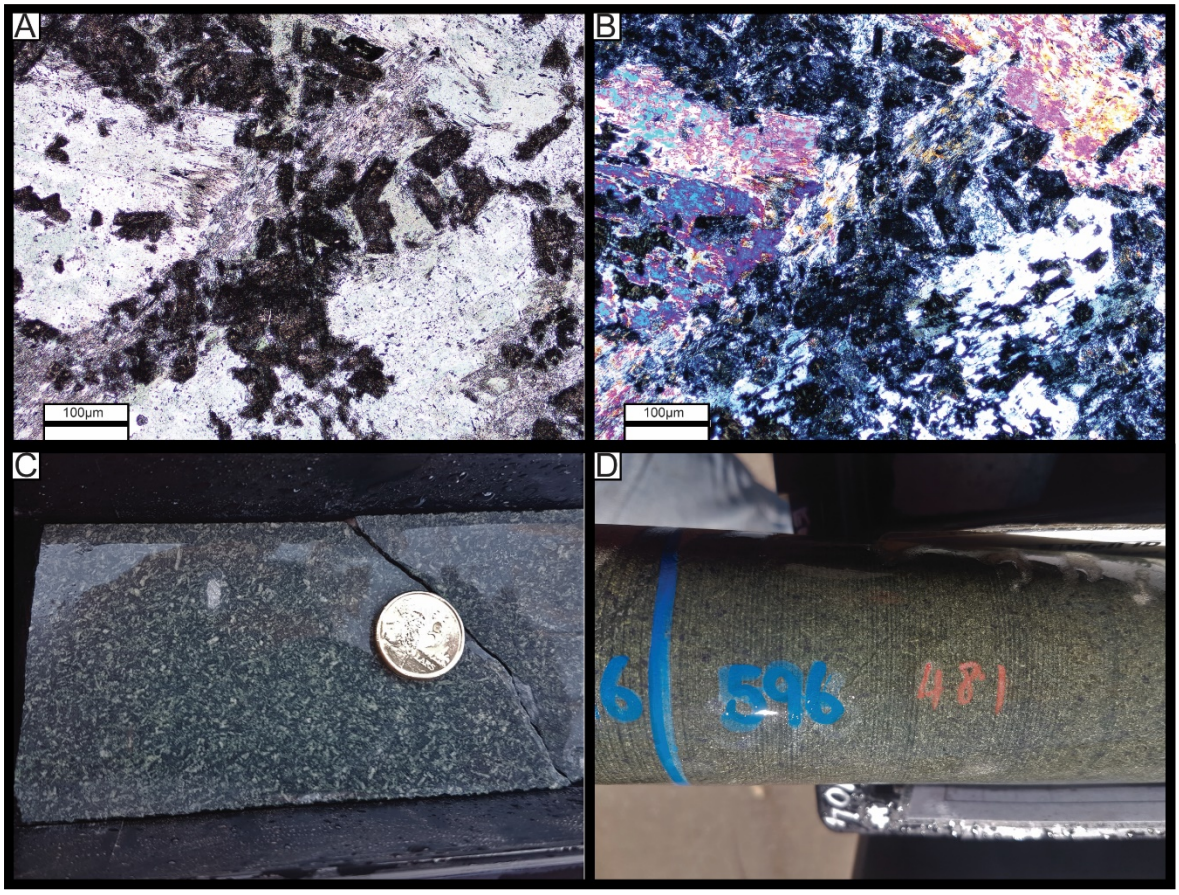

Figure 4.5. A) PPL image of sample 222908 (SE18W1, 1821m) a coherent dolerite which displays a subophitic texture. B) XPL image of sample 222908 note the high birefringence minerals represent the replacement of plagioclase by clinozoisite while the dark tabular minerals represent chlorite replaced pyroxene. C) dolerites of SE19W1 2823m showing variation in alteration leading to the apparent growth of crystals and formation of "leucocratic dolerite". D) Medium-grained Golden Mile Dolerite (JUGD001, 596m)

4.2.4. Quartz dolerite

Description. Medium to coarse-grained (2mm-5mm) quartz-bearing dolerite was only observed within the uppermost sections of the Golden Mile Dolerite within drill hole JUGD011 (830m-1090m) (Fig. 4.6C, D). This unit occurs in contact with the coarse grained granophyric sections of unit 8 described below and the upper dolerites of unit 9, the contact relationships appear the be gradational although they are obscured by heavy alteration. These units share similar mineralogy to the previously described dolerite lithofacies with clinopyroxene and plagioclase feldspar (now albite) being the major primary igneous minerals as well as primary quartz (Fig. 4.6). Small (<2mm) graphitic to granophyric intergrowths of quartz and what was likely alkali feldspar can be seen in this unit, however, abundances of these intergrowth are lower than then later described Granophyre (Fig. 4.8).

A general observation of the quartz dolerites is that they seem to be lighter in colour, however this may be the result of alteration. The quartz dolerites can be distinguished from both the granophyre and dolerites by means of geochemistry (see chapter 5, Fig 5.3).

Interpretation. The quartz dolerites observed in JUGDD011 are interpreted to represent the upper solidification front for a second Ti rich magmatic pulse into the Golden Mile Dolerite (see chapters 5 and 6 for a more detailed description). incorporation of granophyric intergrowths within these rocks may suggest the mixing or possible space in fill of the evolved granophyric material into the solidifying coarse grained upper solidification front (Marsh, 2015). These upper solidification front textures within the centre if the Golden Mile Dolerite align with a differentiating intrusive body which has experienced subsequent magma injections (Marsh, 2015, Marsh, 2002, Zavala et al., 2011).

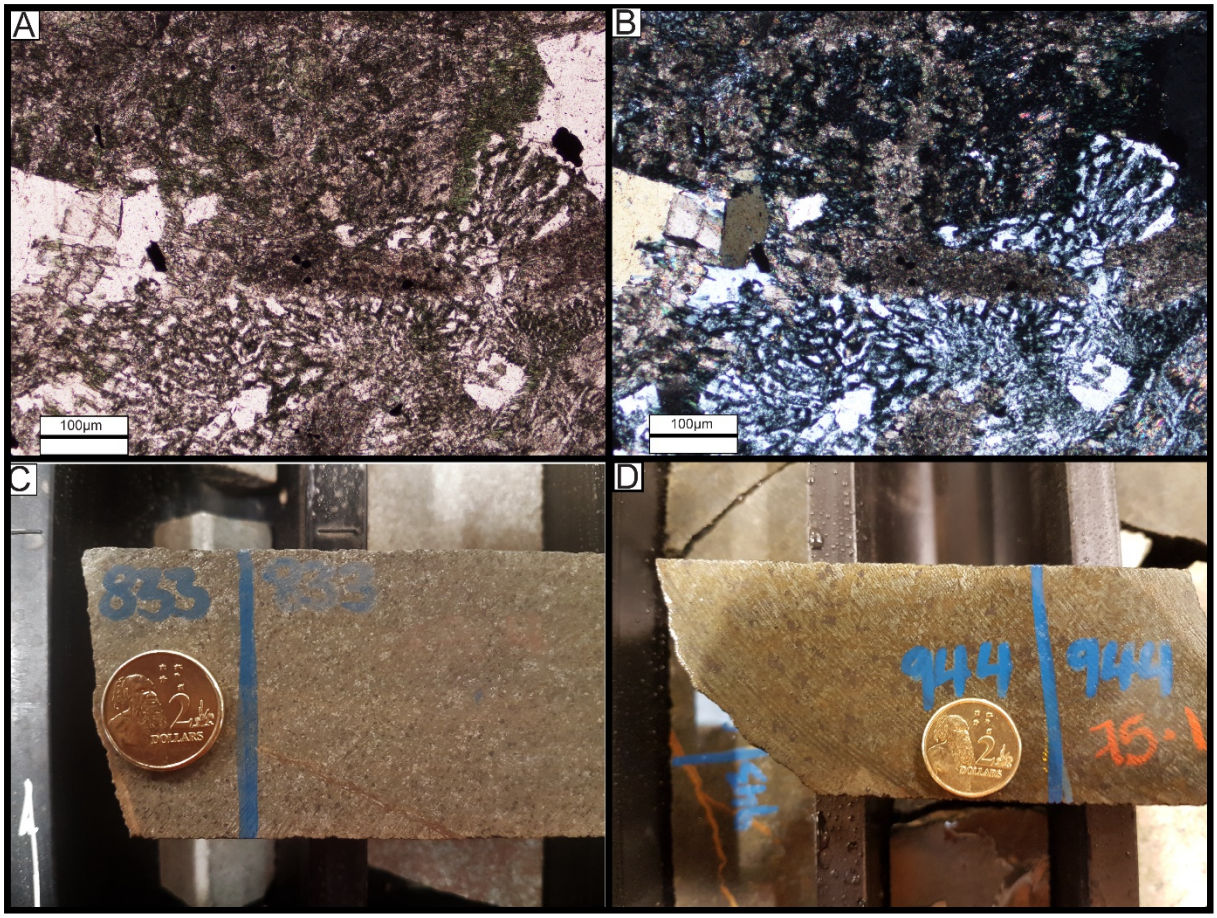

Figure 4.6 A) PPL image of sample 222925 (JUGD011 932m) showing minor granophyric intergrows surrounding altered cristals of clinopyroxene, quartz and plagioclase feldspar. B) a XPL image of sample 222925. C) hand sample of quartz-bearing dolerite proximal to the granophyric segregations (JUGD011, 833m) D) hand sample from within the upper more massive quartz dolerite/ granophyre zone (JUGD011, 944m)

4.2.5. Coherent gabbro

Description. Coarse grained sections of the Golden Mile Dolerite are common within the thicker (>100m) thick intersections. The mineralogy of the gabbroic rocks remains relatively consistent to the previously discussed dolerites with subequal amounts of plagioclase feldspar with pyroxene crystals as well as minor Fe-oxides and minor quartz with the main change being in crystal size (>5mm). Two samples of the SE18W1 gabbro were processed for petrographical work (samples 222906 1763m, 222907 1781m), however, extensive alteration and carbonate replacement has destroyed mineral textures. As discussed above, the apparent growth of minerals resulting from alteration can make the identification of true gabbroic rocks difficult. Like the transition from basalt to dolerite, the contacts of the gabbroic units with the surrounding dolerites are gradational and occur over several metres. Pyroxene rich cumulate sections are common at the bases of thicker dolerite sections (JUGD011 600-645m, SE18 1410-1455m, 1785-1865m) and show oikocrysts of quartz as well as stacked crystal boundaries (Fig. 4.7)

Interpretation. The coarse gabbroic sections of the Golden Mile Dolerite are interpreted to be the result of both a slow cooling fractionating mafic intrusion (Marsh, 2015). The coarse basal pyroxene cumulates are interpreted as the result of gravity driven fractional crystallization and the accumulation of dense mafic crystals (Marsh, 2015).

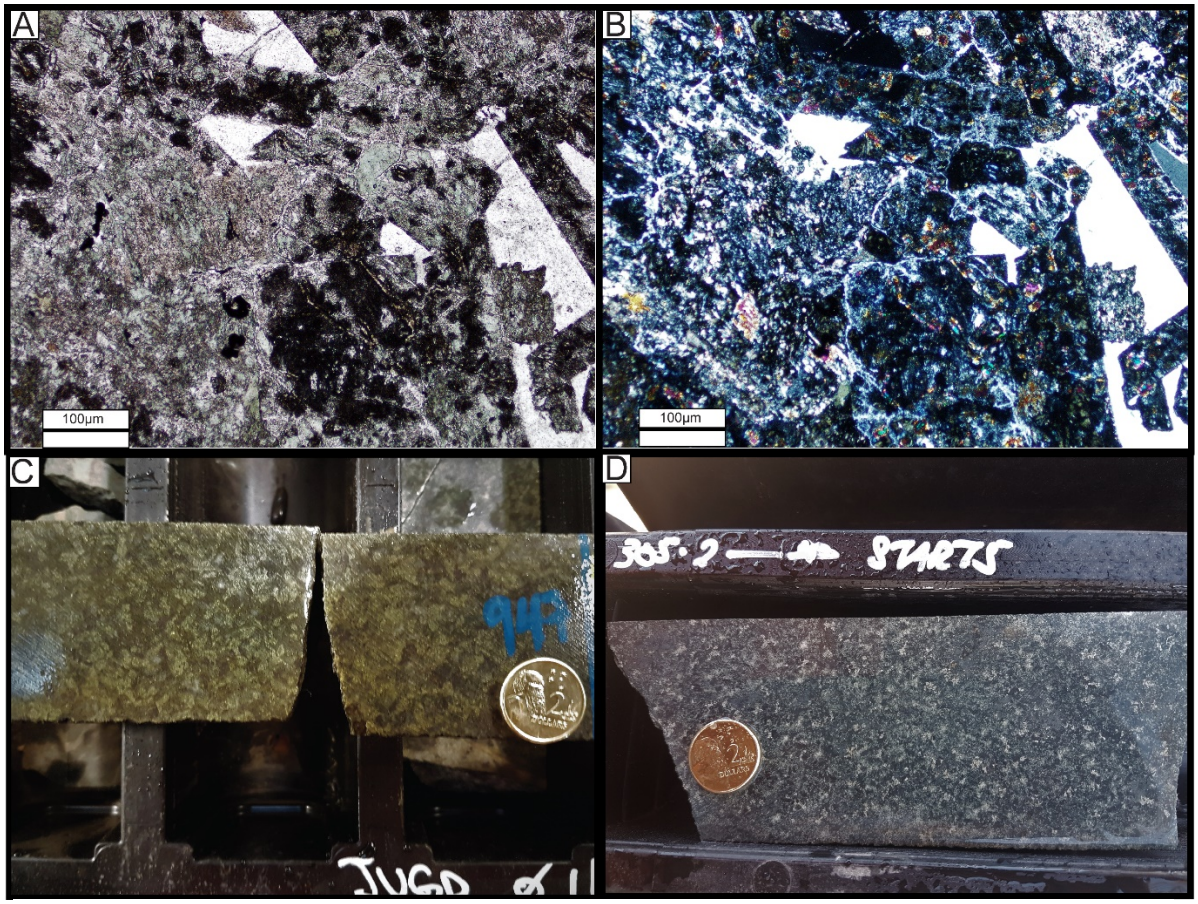

Figure 4.7.A) PPL image of a quartz-bearing dolerite. note the sharp boundaries with the chlorite altered relic pyroxene crystals and well-formed quartz crystals (sample 222918, JUGD011 588m). B) XPL Image of sample 222918, the quartz crystals in the bottom right of the picture share a common extinction angle suggesting a possible overgrowth/ poikilitic relationship. C) Heavily altered gabbro of the Golden Mile Dolerite (JUGD011, 947m). D) An altered basal pyroxene cumulate (JUGD011, 305m).

4.2.6. Silicic segregations

Description. The thickest Golden Mile Dolerite bodies include coarse (>5mm) internal sections of quartz, plagioclase feldspar (now albite), clinopyroxene, subhedral magnetite/ilmenite and distinctive granophyric intergrowths of quartz and what was alkali feldspar (Fig. 4.8A, B). Mesostasis makes up a large proportion of these units (40-60%) which consists of primarily microcrystalline quartz and chlorite (Fig. 4.8 C, D). This facies exists as isolated <1m-5m dyke or sill-like structures within a section of fine grained basalt (JUGD011, 670m-945m. SE19W1, 950-980m, 1260m-1330m, 1490m-1520m, 2530m-2560m) (Fig. 4.8E). The contacts of these units are marked by rapid transitional boundaries from coarse felsic material (>5mm) to fine (1mm) coherent basalt over a few centimetres (JUGD011 670m- 830m) (Fig. 4.8F). These boundaries, when forming in coarser grained

quartz dolerite become more gradational and difficult to distinguish and more massive granophyre/quartz dolerite zones occur (JUGD011 845m-945m). Internally crystals of these silicic segregations appear to nucleate from the contact growing inwards (Fig. 4.8E)

Interpretation. The coarse grained silicic sections of the are interpreted as Granophyric segregations (Marsh, 2015, McDougall, 1964, Zavala et al., 2011). These Granophyric segregations within the fine-grained basalt may be interpreted to be the result of the differentiation dolerite intrusive sill (McDougall, 1964, Marsh, 2015, Zavala et al., 2011). The formation of these segregations will be discussed in greater depth in the discussion chapter 6, however, these segregations likely formed through the separation of the crystal and melt phase (Marsh, 2015, McDougall, 1962, McDougall, 1964). This separation may be driven through differentiation (in-situ or in a lower magma chamber) as a result of gravity or convection driven fractional crystallization leading to a more evolved melt (McDougall, 1964, McDougall, 1962, Travis et al., 1971, McCall, 1973, Marsh, 2015). This separation would also account for the cumulate zones noted at the bottom of the Golden Mile Dolerite (Travis et al., 1971, Bateman et al., 2001). Alternatively, mush flow fractionation or partial melting could also account for the formation of these granophyric segregations in the suggested multiple pulse system of the Golden Mile Dolerite (Marsh, 2015, Travis et al., 1971, McCall, 1973). The rapid change from coarse granophyre to fine basalt seen in DDHJUGD011 (670m- 830m) (Fig. 4.8 F) may suggest that the differentiated felsic source fluids were injected into this fine-grained basalt or possibly as the result of these granophyric segregations rising though the unsolidified magma through solidification front instability (Marsh, 2002, Marsh, 2015, Zavala et al., 2011).

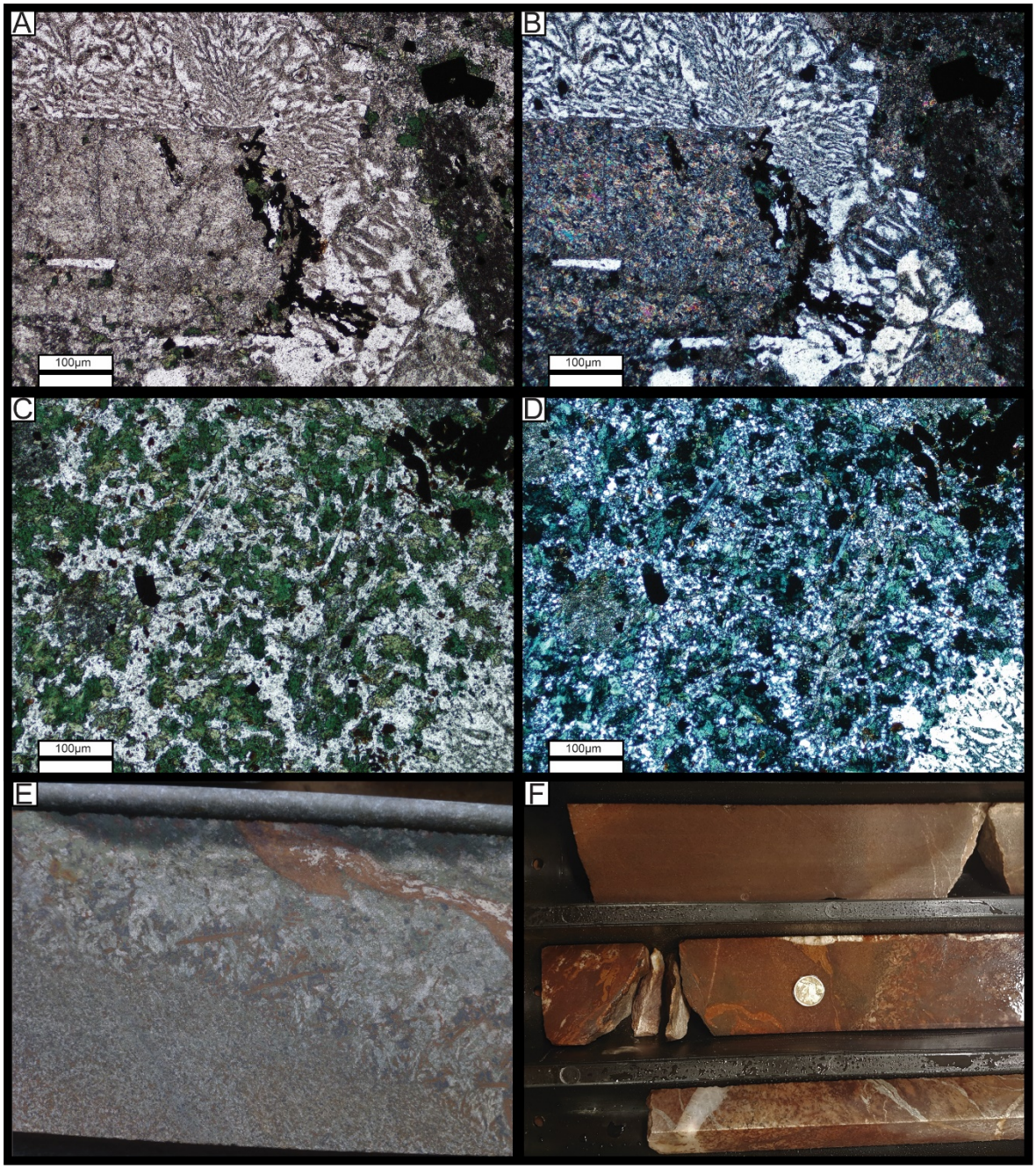

Figure 4.8 A) Sample 222931 PPL image of a relic tabular plagioclase feldspar crystal now clinozoisite (left) surrounded by granophyric intergrowths of quartz and feldspar. B) XPL image of 5.A. note dark crystal in right is likely a heavily chlorite altered relic pyroxene crystal with internal crystallization of blocky secondary magnetite (opaque). C) Sample 222931 PPL image of the abundant mesostasis associated with the granophyric zones consisting almost entirely of microcrystalline quartz and chlorite. D) XPL image of 5.C. E) image of granophyre segregation from JUGD011. F) The rapid transition from fine-grained basalt to coarse granophyre over a few centimetres.

4.3. Other coherent facies of the Kalgoorlie Domain

4.3.1. Hornblende porphyry

Description. Thin (>1m-2m) fine-grained chlorite altered igneous dykes intrude the Golden Mile Dolerite in several places JUGD011 (530m – 550m), SE19 (773m, 780m 800m,855m) TRGD0011 (245m) (Fig. 4.9 C, D). Unlike the dolerites of the Golden Mile Dolerite this unit shows a textural alignment of grains with a pervasive fabric throughout the sample, however, this may be due to localized deformation. The mineralogy of the dykes is defined by a fine-grained groundmass, later altered to chlorite/epidote/carbonate with relic euhedral crystals of hornblende and fibrous actinolite (Fig. 4.9 A, B).

Interpretation. The geochemistry and mineralogy of these rocks suggest that they represent some of the more felsic porphyritic dykes found within the Kalgoorlie domain (O'Connor-Parsons and Stanley, 2007). This dyke, by intruding the Golden Mile Dolerite, therefore, must postdate the intrusion of the Golden Mile Dolerite and will not constrain the emplacement of the Golden Mile Dolerite.

Figure 4.9. A) PPL image of a relic hornblende crystal within a fine altered groundmass sample 222916 (JUGD011, 531m), B) XPL image of sample 222916 showing the replacement of hornblende. C) An intrusive boundary between the hornblende porphyry (HBP) and the Colden Mile Dolerite (DO) (JUGD011, 530m). D) multiple dykes of hornblende porphyry (HBP) intruding the Golden Mile Dolerite(HBP) (TRGD001, 245m).

4.3.2. Pillow basalts

Description. Pillows are a common feature of the underlying basaltic flow units of the Paringa and Devon Consols Basalt as well as the previously mentioned Eureka Basalt (Hugh Smithies GSWA) (Fig. 4.10 A) and as a result are not generally relevant to this study (Said and Kerrich, 2010, Said et al., 2010, Said and Kerrich, 2009, Travis et al., 1971). However, within the uppermost sections of drillhole SE19 (233-282m) approximately 50m of lobate structures with hyaloclastite margins are found at the top of the main dolerite unit. These lobate structures are irregular in shape and show altered heavy chloritoid alteration as well as possible altered rims (Fig. 4.10 B). The lobate structures seen in SE19 seem to sit at a higher stratigraphic level than those in SE18W1 and lack a distinct sedimentary boundary separating them from the lower dolerite units as well as missing a distinct upper boundary with overlying Black Flag Group.

Interpretation. The pillowed structures observed below the Golden Mile Dolerite within SE18 Have been interpreted as representing subaqueous basaltic flows with the more massive sections representing sheeted flows of the underlying basaltic flows of the Eureka and Paringa Basalts (Said and Kerrich, 2010, Said et al., 2010, Chadwick et al., 2013, Clague et al., 2013, Fundis et al., 2010). The lobate structures observed in SE19 however are unclear in their form and may represent either the pillowed flows of an extrusive unit or possibly the lobate contacts of a pillowed sill (McPhie et al., 1993, Kano, 1991).

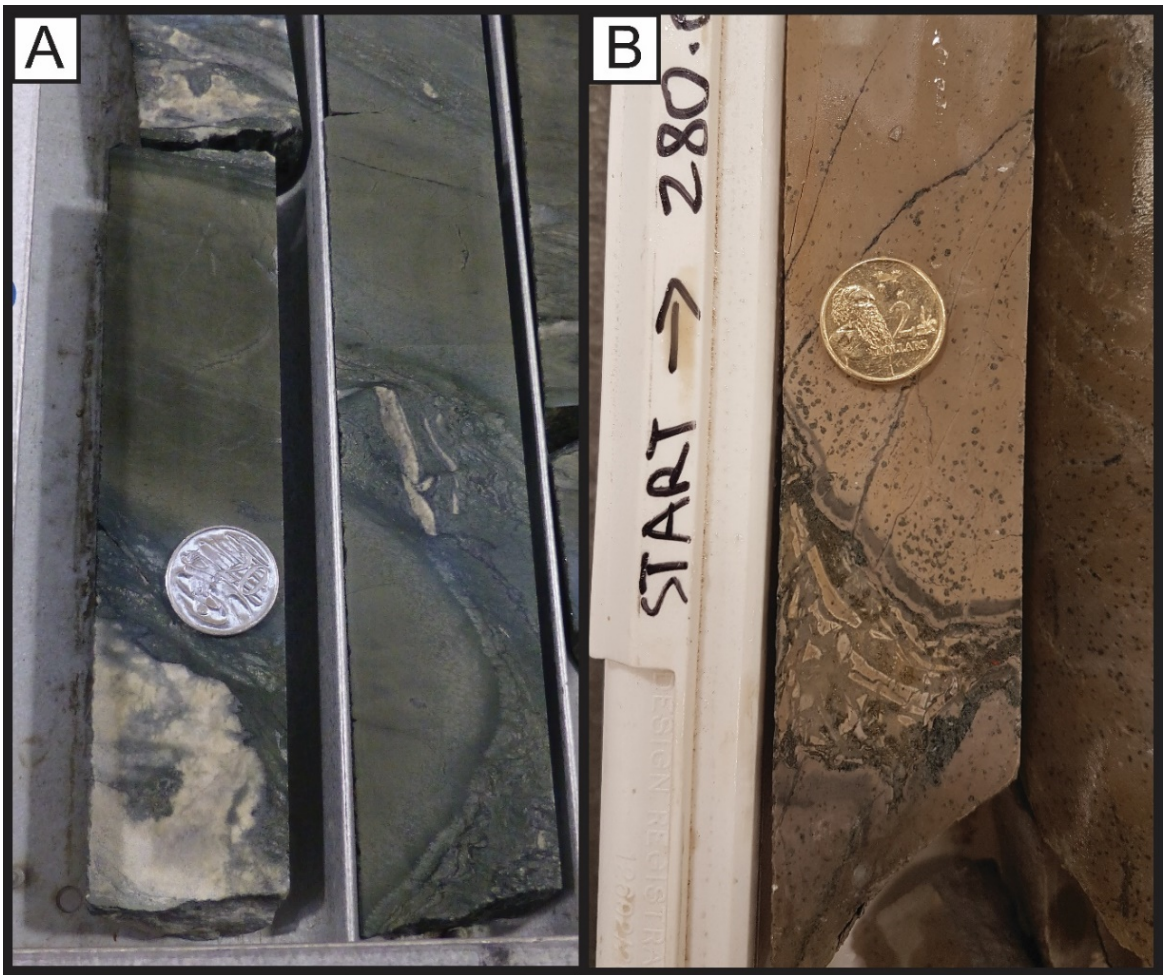

Figure 4.10 A) Pillows of the Paringa Basalt showing ghosted alteration margins and hyaloclastite material (SE18, 2033m). B) Possible heavily altered pillowed basalts showing large blocky hyaloclastite margins and black chlorite alteration rims and perversive chloritoid alteration (SE19 280m)

5.0. Geochemistry

5.1. General classification

The mafic rocks of the Golden Mile Dolerite span a range in lithologies from mafic cumulates, to proper basalts, dolerites, and fine-grained gabbros, through to granophyric segregations. These are chemically variable from picobasalts to basaltic andesites, but plot predominantly in the basalt field on a total alkali versus silica diagram (Maitre, 1989)(Fig.5.1). Of the 132 whole-rock geochemical samples analysed from drill holes SE18 and JUGD011, 73 were collected from the Golden Mile Dolerite, 29 from the underlying basaltic flows and 30 from the adjacent volcanoclastic units of the Black Flag Group The surrounding units sampled are also plotted on the TAS classification diagram (Fig. 5.1), however, due to the focus of this project on the Golden Mile Dolerite, these other stratigraphic units will not be discussed in detail. It is important to note that the rocks of the Kalgoorlie stratigraphy have experienced variable amounts of primarily epidote, chlorite, and carbonate alteration, and as a result some fluid-mobile elements will most likely have disrupted values and should be viewed with caution.

5.2. Geochemically distinct units of the Golden Mile Dolerite

The Golden Mile has been recognised as comprising of 10 distinct geochemical units (Fig. 5.7) by Travis et al. (1971). The upper (9-10) and lower (1-5) units have been previously interpreted to represent a single related magmatic source, separated by a series of two subsequent, differentiated pulses (units 6-7 and 8) (McCall, 1973, Travis et al., 1971). The geochemical samples in this study have been separated into their associated units based on observations made during graphic logging and associated geochemical trends compared to the units of Travis et al. (1971) (Fig. 5.6).

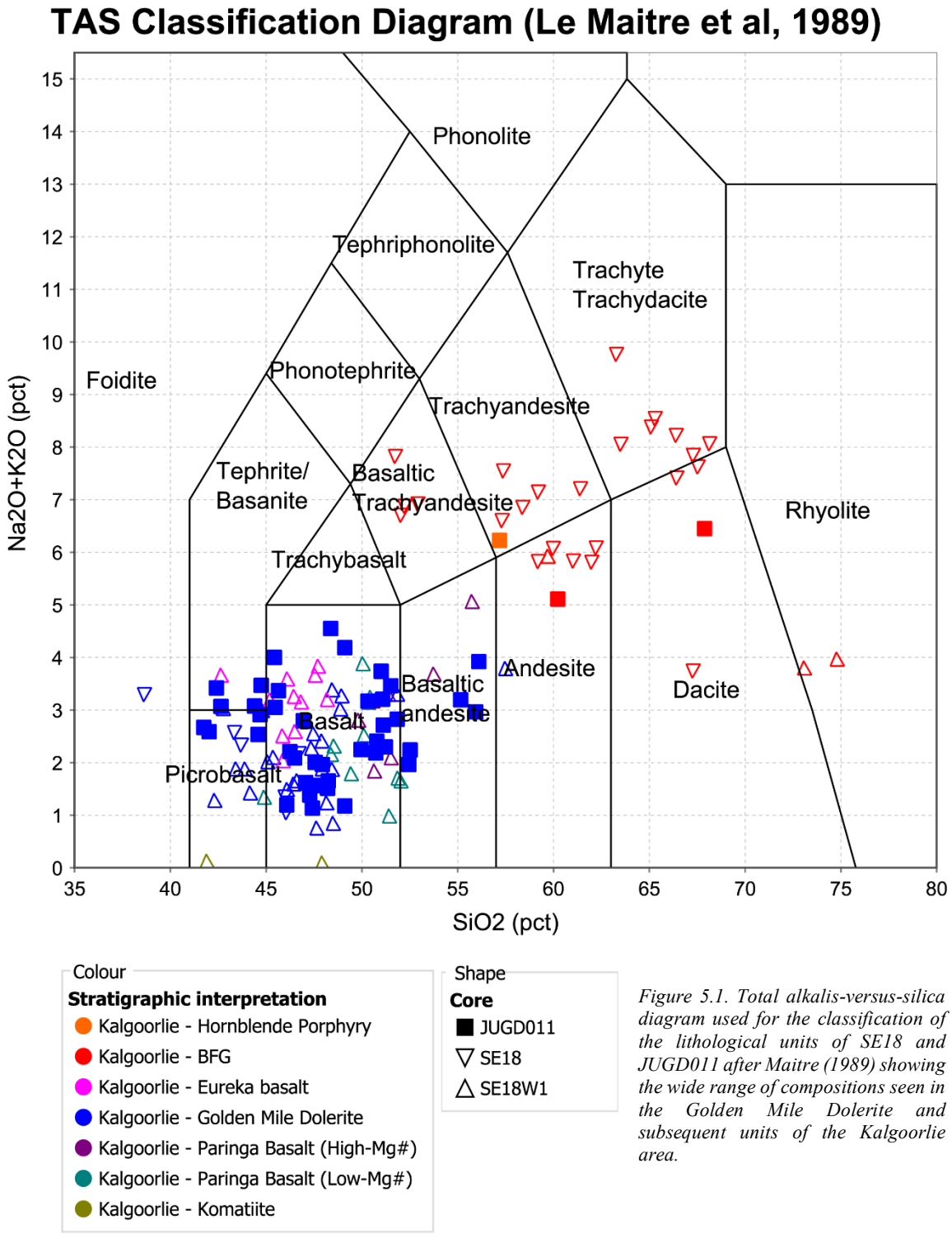

Figure 5.1. Total alkalis-versus-silica diagram used for the classification of the lithological units of SE18 and JUGD011 after Maitre (1989) showing the wide range of compositions seen in the Golden Mile Dolerite and subsequent units of the Kalgoorlie area.

5.3. Major and trace element geochemistry of the Golden Mile Dolerite

Major element oxides and trace elements for the Golden Mile Dolerite are displayed in Figures 5.2 and 5.3, respectively. The major mineral phases of the Golden Mile Dolerite that will affect the chemical trends include clinopyroxene, orthopyroxene, quartz, plagioclase feldspar, magnetite/titano-magnetite, and ilmenite. Negative correlation of Mg with Zr and Nb suggest the accumulation of these incompatible elements through fractional crystallization of pyroxene phases from the melt (partition coefficients for Zr and Nb into clinopyroxene, Zr D=0.043–0.18, Nb D=0.0006–0.0067 after (Green et al., 2000)). Although Zr can be compatible into pyroxene, the bulk composition of the melt would lead to overall incompatible behaviour in the rock (D_{Bulk}) Nb, when plotted against TiO_2 shows a separation between the outer units 1-5 and 9-10 from the central units 6-8 (Fig. 5.3). Trends for the increasing immobile elements Zr, Nb, Ta and Sc with decreasing Mg suggests a differentiating basalt magma source, concentrating incompatible elements while becoming more felsic (Marsh, 2015).

5.3.1. Major and trace element geochemistry of the GMD geochemical units.

5.3.1.1. Units 1-5

Located at the bottom of the Golden Mile Dolerite body intersected in JUGD011 and in the basal sections of the lower dolerite unit of SE18 (1750-1850m). This group of rocks is marked by high MgO, CaO and Ni suggesting that these are the most mafic rocks of the GMD, which is reflected in the basal pyroxene cumulates of this group (units 2-3). The rocks of these units show relative depletion in Fe_2O_3, TiO_2 and Nb when compared to the central units (6-8) (Fig. 5.2, 5.3).

5.3.1.2. Unit 6

Occurring at the interface between the feldspar phyric dolerites of unit 5 and the fine basalts of unit 7 this doleritic unit is distinguished by the appearance of magnetite. The change between unit 5 and 6 can be seen both in hand sample as well as geothermally with the enrichment in Fe_2O_3, Ti and most notably Cu (Fig. 5.2, 5.3).

5.3.1.3. Unit 7

This unit consists of fine grained basalts with intermittent granophyric segregations which are associated with unit 8. These rocks are marked by high Fe_2O_3 and Ti values with relative depletion in Cu, Ni and SiO_2 (Fig. 5.2, 5.3).

5.3.1.4. Unit 8

The granophyric segregations rocks of unit 8 show enrichment in wide range of elements and element oxides including SiO_2, Fe_2O_3, Zr and Nb while being depleted in MgO, CaO. These trends suggest that these granophyric segregations are more evolved with a felsic composition. The upper quartz dolerites, when compared to the granophyric segregations can be distinguished by their enrichment in TiO_2 as well as lower Sio_2 values (Fig. 5.2, 5.3).

5.3.1.5. Units 9-10

Units 9 and 10 share similar geochemical trends with units 1-5 which can be seen when Nb is plotted against TiO_2 showing a clear geochemical relationship. This relationship is reinforced by the consistently similar trends when these units are plotted together eg., TiO2, SiO2, CaO P2O5, Al2O3, Zr, Nb and Cu. The strong geochemical similarities between units 1-5 and 9-10 suggest that they are genetically related as described by (Travis et al., 1971, McCall, 1973) (Fig. 5.2, 5.3).

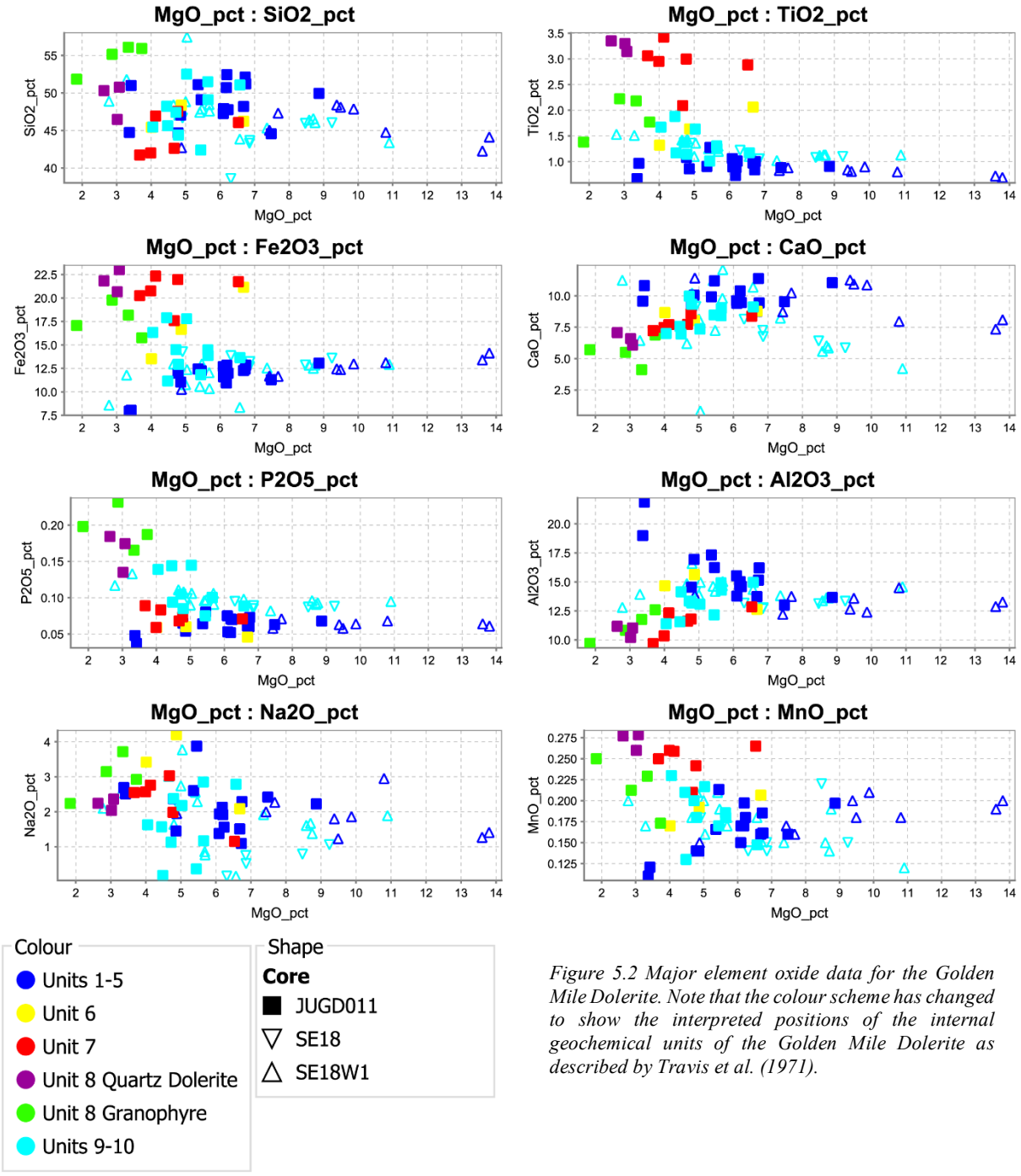

Figure 5.2 Major element oxide data for the Golden Mile Dolerite. Note that the colour scheme has changed to show the interpreted positions of the internal geochemical units of the Golden Mile Dolerite as described by Travis et al. (1971).

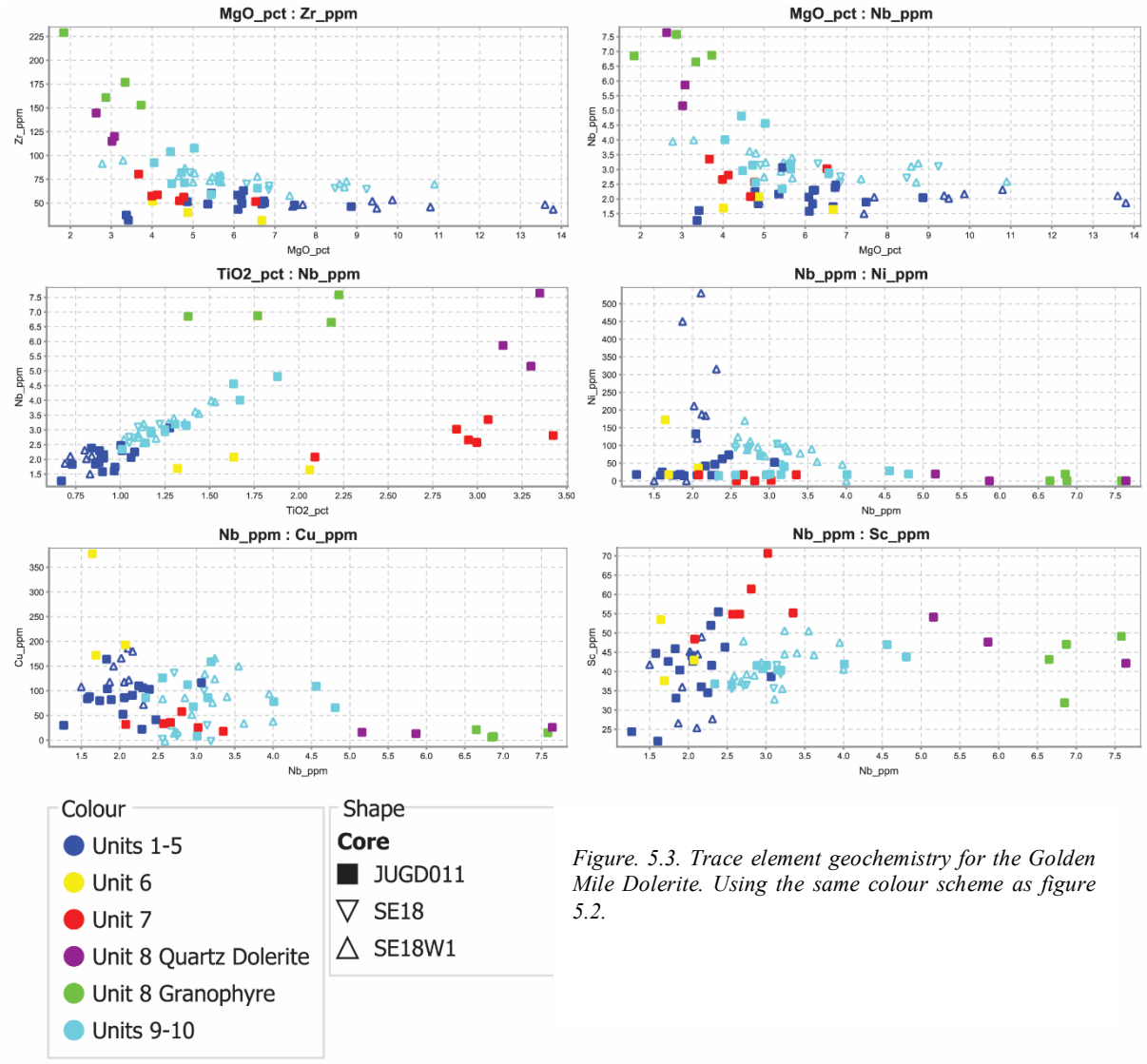

Figure. 5.3. Trace element geochemistry for the Golden Mile Dolerite. Using the same colour scheme as figure 5.2.

5.4. Drill holes and down hole geochemistry

5.4.1. SE18

The drill holes that the geochemical data for this study were obtained (SE18, JUGD011) intersect markedly different exposures of the Golden Mile Dolerite. Drill hole SE18 is drilled in a distal section of the Golden Mile Dolerite (Fig. 2.2) and intersects two smaller dolerite bodies separated by the mudstones and sandstones of the Black Flag Group. The upper and lower dolerite bodies of SE18 are relatively thin when compared to JUGD011 at approximately 100m and 200m observed thickness, respectively. Both intrusions coarsen from aphyric basalt to dolerite/gabbro towards the bottom third of the body with a thin 2–15 m zone of basalt on the contact with the underlying unit (Fig. 6.1.). Multiple thin basaltic units occur in the overlying and underlying sediments of the Black Flag Group which are

geochemically the same as the major dolerite units (Fig5.3) The smaller upper dolerite body is poorly represented with only six points across the >100 m body at disproportionate spacing (Fig. 5.4) Geochemical trends can still be seen with this data with stable data for Ti/Zr, V and Fe_2O_3 values as depth increases, these trends are accompanied by Mg values that sharply increase towards the base of the body (Fig. 5.4). The spike in Mg at the base of the unit is consistent with the formation of a pyroxene cumulate, as is seen in the increased grain size observed during logging (Fig. 6.1.) Data coverage for the larger intersection of the Golden Mile Dolerite in SE18W1 is much more comprehensive and appropriately spaced then its SE18 counterpart. The mafic rocks of this section show similar stable Ti/Zr, V and Fe_2O_3 values compared to SE18 as well as the noted spike in magnesium associated with the bottom third of the body (Fig. 5.4.). The basal clinopyroxene cumulates of SE18 show spikes in Mg concentrations while Fe_2O_3 remains relatively stable, this may indicate that the clinopyroxene incorporated in these cumulates is of a Mg rich endmember possibly Mg rich pigeonite or augite.

5.4.2. JUGD011

JUGD011 occurs in a thick central section of the Golden Mile Dolerite proximal to the Fimiston Pit (Fig. 2.2). Drilled from oldest to youngest, the stratigraphy and collared within the lower units of the Golden Mile Dolerite JUGD011 intersects almost entirely Golden Mile Dolerite with the hole terminated after the top contact with the Black Flag Group sedimentary rocks. This drill hole intersects the majority of the internal geochemical units defined by Travis et al. (1971) (units 2–10) with the exception of the basal chilled marginal basalt (unit 1) (Fig. 5.4,5.6., 5.7). Downhole geochemical plots were made for the two aforementioned drill holes using selected element ratios, trace elements and element oxide data, to attempt to match the trends reported by Travis et al. (1971); (Fig. 5.4). For this study, the Golden Mile Dolerite observed in SE18 and JUGD011 were subdivided into six subsections based on the 10-unit system. These units were adapted to represent the interpreted pulses of more differentiated/Fe-rich magma as described by(McCall, 1973, Travis et al., 1971). In this system Units 1-5 (lower) and 9-10 (upper) have been generally grouped as they are geochemically similar (Fig. 5.3) while the central units 6, 7 and 8 have been separated into individual groups to show them as geochemically unique units. this subgrouping has been extended to separate unit 8 into two sub categories of true granophyre

and quartz dolerite based on chemical and possible source differences (Fig. 5.3) (see discussion for detailed explanation). JUGD011 gives a comprehensive geochemical cross-section of the thickest section of the Golden Mile Dolerite observed in this study while also showing a range of geochemical trends. Geochemical trends for units 1-5 show relatively flat trends for Ti/Zr and V with a sharp increase in all plotted element data at the intersection with unit 6 (595m). These chemical trends are broadly repeated at the top of the body in units 9-10. Fe_2O_3 values increase steadily (approx. 12-20 wt%) from the top to the bottom of unit 9 (900m) where they remain relatively high until the base of unit 6 when values rapidly decrease (approx. 24-15 wt%). Mg values for the base of the JUGD011 show a similar trend to both SE18 and SE18W1, with a spike in Mg gradually decreasing towards the top of units 1-5. Geochemical data from the central units (6-8) show sporadic trends for Ti/Zr and V with the granophyric and quartz doleritic rocks showing depleted anomalies. The quartz doleritic rocks of unit 8 show minor enrichment in Mg and Fe_2O_3 while the granophyric rocks of the same unit show depleted values, all of unit 8 is distinguishable by its major depletion in V. Units 6-7 show high Ti/Zr values while being slightly enriched in V (Fig. 5.4). The spike in elements observed in unit 6 of JUGD011occurs as medium-coarse grained dolerite/ clinopyroxene cumulate and may represent a settling zone for the fractionation of units 6 and 7

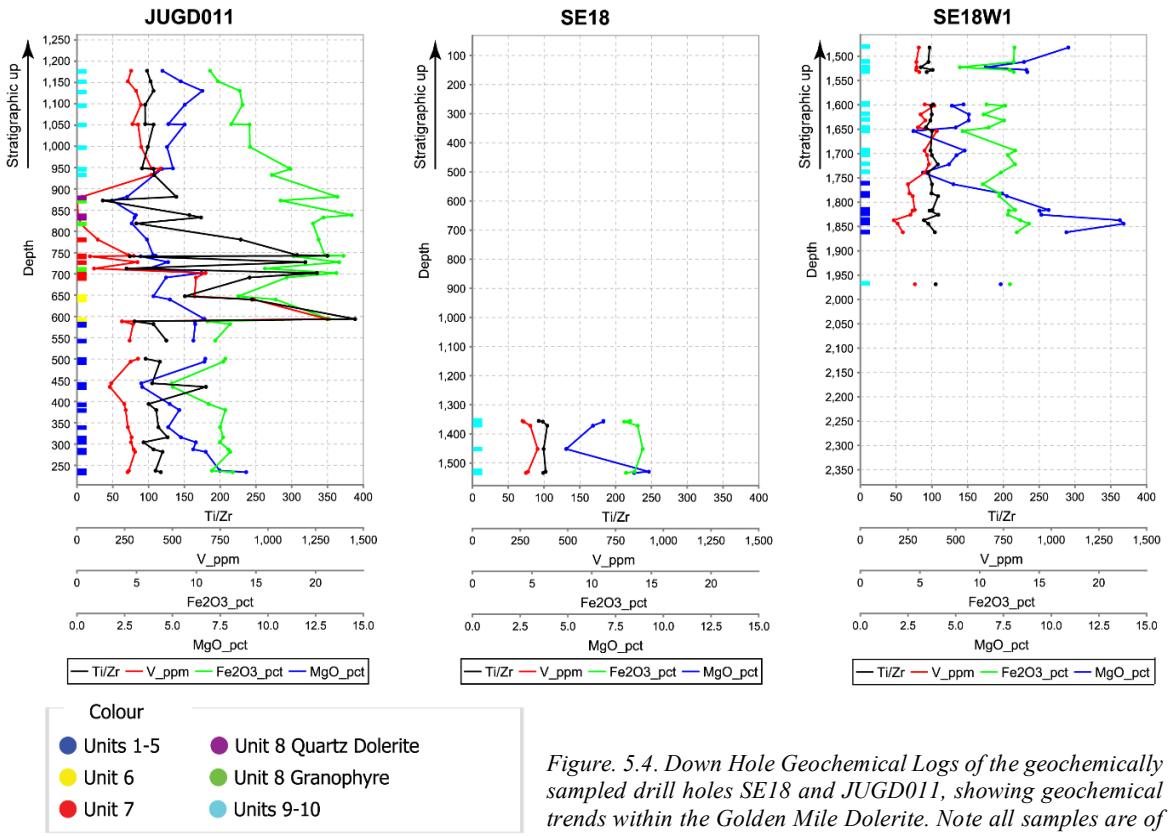

Figure. 5.4. Down Hole Geochemical Logs of the geochemically sampled drill holes SE18 and JUGD011, showing geochemical trends within the Golden Mile Dolerite. Note all samples are of the GMD and the colours represent the interpreted 10 geochemical units as described by Travis et al. (1971). Drill hole JUGD011 has been overturned orientate bottom of the hole as the top the top of stratigraphy.

5.5. Thorium (Th) basalt grouping

The basaltic rocks of the Eastern Goldfields superterrane have also been separated into three geochemically distinct groups on the basis of Th as well as other immobile and REE geochemistry (Barnes et al., 2012). The Paringa basalt is of the high Th silicious basalt group (HTSB), the Devon Consols basalt is of the intermediate Th basalt group (ITB), and the Lunnon basalt and Golden Mile Dolerite are of the low Th basalt group (LTB) (Barnes et al., 2012). The observed trends match well with the expected results as the Paringa Basalt plotted within the HTSB and the Golden Mile Dolerite generally plotted within the LTB. Samples of the GMD from SE18, when plotted in as TiO_2 vs Th (Fig. 5.5.), show several anomalously high Th samples (211557, 222905,222906 and 222924) (see digital appendix). This would suggest that these rocks are of an ITB composition rather than LTB. These samples occur over both drill holes with only samples 222905 and 222906 occurring in the same upper basaltic section of the second dolerite body in SE18 (SE18W1 1739.03 and

1763.03 respectively), while sample 211557 occurs as a thin basaltic unit below the upper dolerite body in SE18 (SE18 1522.71 m) and 222924 from the centre of unit 7 (JUGD011, 872.525m). These anomalous data points may be the result of analytical error as they generally plot with the other Golden Mile Dolerite samples when plotting against other trace elements (Fig 5.5).

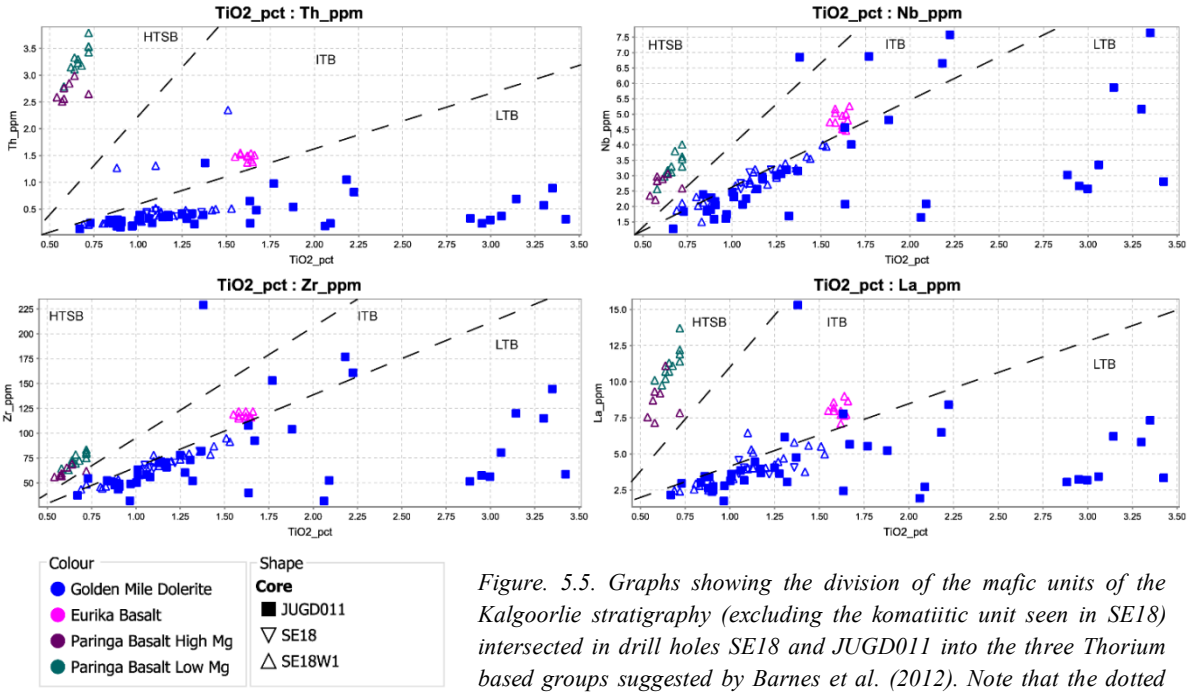

Figure. 5.5. Graphs showing the division of the mafic units of the Kalgoorlie stratigraphy (excluding the komatiitic unit seen in SE18) intersected in drill holes SE18 and JUGD011 into the three Thorium based groups suggested by Barnes et al. (2012). Note that the dotted lines are illustrations to roughly show groupings and are not calculated lines.

5.6. **Summary**

The Golden Mile Dolerite is a geochemically diverse mafic body which ranges from basaltic-andesitic felsic segregations to mafic/ultramafic cumulate units. the samples of SE18 and JUGD011, when compared to the geochemical trends of Travis et al. (1971) (Fig. 5.6, 5.7) generally matched their observations. Comparing SE18 to JUGD011 showed that the central units 6-8 were absent from the sampled intersections while correlating the sampled basalt and dolerite to units 1-5 and 9-10 (Fig. 5.3). The separation of two geochemically similar groups (1-5, 9-10) by a body of geochemically distinct mafic rocks suggest that multiple magmatic pulses are responsible for the formation of the Golden Mile Dolerite and its internal geochemical units. When subdivided into Th basalt groups the Golden Mile Dolerite

samples generally plotted within the Low Th group as expected (Barnes et al., 2012) although several outliers are present and their relationship is unclear (Fig. 5.5).

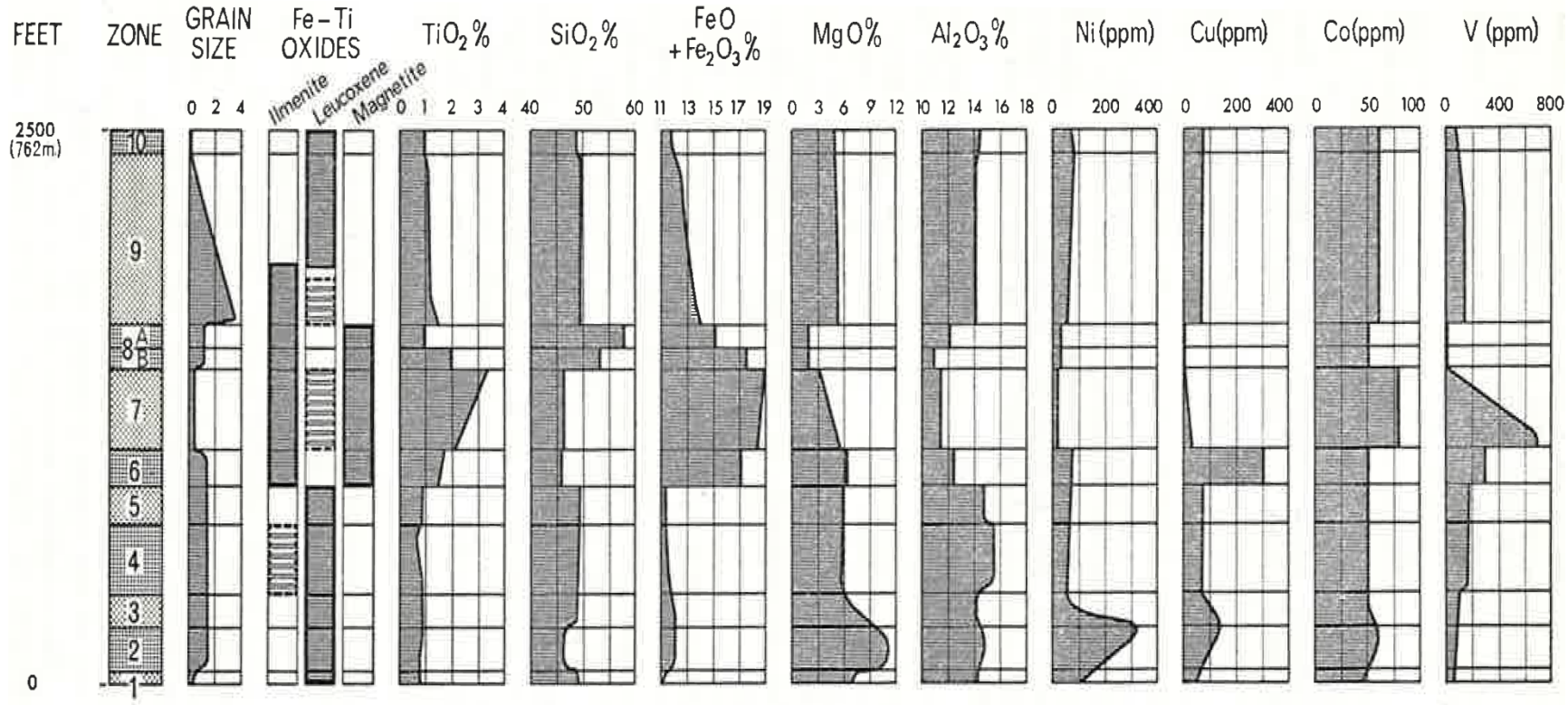

Figure 5.6. geochemical trends of the 10 units of the Golden Mile Dolerite (Travis et al., 1971)

Geochemical Unit	Thickness	Primary Mineralogy	Magnetite	Description
10 - Upper chilled basalt margin	10m	Opx-ox-Pl	N	Fine grained-aphyric basalt, can be variolitic
9	100-300m	Thought to represent the reversed telescoped equivalentt of Units 2-7		
8	100-200m	Cpx-ox-qz-Pl	Y	Granophyric rather than Doleritic with eutectic intergrowths of what is now albite-quartz
7	100-200m	Pl-ox-2px	Y	Fine gained subophitic dolerite/basalt with thin internal granophyric segregations
6	<100m	Pl-ox-2px-qz	Y	Medium grained dolerite, Similar to U5 but marked by appearance of magnetite and ilmenite
5	<100m	Pl-2px-qz-ox	N	Medium grained subophitic plagioclase phyric dolerite
4	90m	Tabular opx-cpx-ox-pl	N	Medium grained pyroxene-phyric dolerite
3	40m	Tabular opx-cpx-ox-pl	N	Small basal pyroxene cumulate grading into into a top of medium grained dolerite
2	30-60m	Platty opx-cpx-ox	N	Ultramafic unit, Coarse pyroxene cumulate and the only unit with no primary Quartz
1 - Lower chilled basalt margin	10m	Opx-ox-Pl	N	Fine grained-aphyric basalt, can be variolitic
Opx - Orthoproxene	Ox - Fe/Ti oxides	Cpx - Clinopyroxene	Qz - Quartz	Pl - Plagioclase Feldspar

Figure 5.7. A summary table of the 10 units described by Travis et al. (1971) showing the mineralogy and textures of each unit, modified from Bateman et al. (2001)

6.0. Discussion

6.1. Introduction

In this chapter, the field, petrographic and geochemical results of chapters 3-5 will be discussed with the intent of interpreting the mode of emplacement of the Golden Mile Dolerite. These results will be used to compare the predominant models of a traditional post-depositional intrusive sill against an extrusive thick ponded lava sequence while offering an alternative syn-depositional intrusive model based on new observations made during this study. When evaluating the evidence collected it is important to take into account to some degree, the Archean setting and the level of uncertainty in the processes occurring at this time.

6.2. Environment and timing

To give context to these processes the environment into which the Golden Mile Dolerite was emplaced and the associated textural implications, will be summarised. The older underlying pillowed and sheeted basaltic flows of the Paringa and Eureka Basalts suggest a subaqueous environment (Chadwick et al., 2013, Clague et al., 2013). This is supported by the thick black mudstones and turbidite sequences of the encompassing Black Flag Group (Henrich and Hüneke, 2011, Hüneke and Henrich, 2011, Mulder et al., 2011). Evidence of subaerial volcanism has also been recognised higher in the Black Flag Group stratigraphy, with the presence of andesitic mass flow breccias (Fig. 4.2) which abruptly overlie the black mudstones of the Black Flag Group. This observation is similar to observations made by Squire et al. (2010).

The age of the Golden Mile Dolerite and its surrounding units is important in understanding the possible depositional environments that may have existed. U-Pb dating conducted by Rasmussen et al. (2009) on zirconolite and xenotime grains within the Golden Mile Dolerite give an age of 2680 ± 9Ma. The andesitic breccias, volcanic sandstones and mudstone beds encompassing the Golden Mile Dolerite represent the lower extents of the Early Black Flag Group of which a basal dacitic clast has been dated at 2686 ± 3Ma (Krapez et al., 2000). The depositional age range for the Early Black Flag Group and Golden Mile Dolerite show significant overlap. This overlap allows for the Golden Mile Dolerite to potentially be

emplaced prior to deposition of the overlying Black Flag Group sediments, as simultaneous depositional events or to have been emplaced as post-depositional deposits. Each of these scenarios would result in their own unique emplacement style and deposit characteristics, each of which will be discussed in detail below.

6.3. Contact relationships

The most important observations when differentiating between an intrusive and extrusive origin are those of the contact relationships.

6.3.1. Extrusive conditions

For a basaltic extrusive origin in this proposed submarine environment, the lava flows should be marked by pillowed basaltic upper sections possibly accompanied by massive sheet flows lower in the sequence (Chadwick et al., 2013). The top contact of this extrusive flow would display a conformable relationship with the overlying sediments as well as the production volumes of hyaloclastite at the top of the lavas including possible pillow breccias, and peperite at the base of the lavas (Dimroth et al., 1978, van Otterloo et al., 2015b, Chadwick et al., 2013, McPhie and Cas, 2015).

6.3.2. Intrusive conditions

In contrast, the contact relationships of intrusions into solid rock would display sharp or undulating slightly discordant contacts if a sill, or cross-cutting relationships with the host rock if a dyke (Marsh, 2015). Chilled top and bottom margins of the intruding body are common as the hot magma enters the cool host rock while inversely contact metamorphism may alter the host rocks which have been intruded (Hanson, 1995, Marsh, 2015). In contrast, a syn-depositional intrusion into unconsolidated wet sediments would display a unique contact relationship in the form of top and bottom peperitic margins (White et al., 2000, van Otterloo et al., 2015b). These contacts would show a mixture of hyaloclast fragments of chilled magma mixed into a matrix of surrounding sediments, with bedding and other sedimentary structures being destroyed in the process (White et al., 2000)(see literature review for a more in detail review of these contact textures). Magma-unconsolidated wet sediment interaction may also be marked by the presence of lobate or interfingering

apophyses intruding the sediment both above and below the intrusion (Kano, 1991, McPhie et al., 1993).

6.4. Drill hole correlation

The four graphicly logged drill holes (SE18, SE19, TRGD001 and JUGD011) of this study are compared in figure 6.1. These comparisons show a wide range in thickness from distal hole SE18 to proximal hole JUGD011. Correlations between the top contacts of the Golden Mile Dolerite intersections in these holes has been inferred in figure 6.1 as dashed lines. The top contacts of these units with the possible exception of SE19 all show a similar black mudstone matrix supported breccias.

6.4.1. Evidence from SE18

SE18 consists of two main dolerite bodies with intermittent thin (<10m) basaltic units in the intervening Black Flag Group mudstones. This drill hole shows the widespread development of mudstone supported angular basaltic breccias containing clasts of the Golden Mile Dolerite at both the top and bottom contacts of the major and minor basaltic bodies (see lithofacies descriptions for more detailed description). Breccias of this nature have been interpreted to represent the product of magma-wet sediment interaction as peperitic margins due to the destruction of bedding and apparent sediment-hyaloclast mixing during quench fragmentation (McPhie et al., 1993, Busby-Spera and White, 1987, Kokelaar, 1982, White et al., 2000). In addition to peperitic margins, cross-cutting and interfingering relationships occur between both the larger doleritic bodies/thin basaltic units and the surrounding Black Flag Group sedimentary units, suggesting an intrusive origin, in which thin mafic units, which can be <10cms thick, are interpreted as apophyses (Marsh, 2015). Geochemical data show that these smaller basaltic intrusions are chemically identical to the main bodies and likely represent thin branching apophyses from the main dolerite bodies during the intrusion. In the same way that the basaltic apophyses branch from the larger intrusions, the large intrusions likely represent the branching of the main dolerite body. This proposed branching of the intrusion is supported by the distal location and thinning of the intrusions suggesting this location may be closer to the advancing front of the intrusion (Marsh, 2015). From these observations, the Golden Mile Dolerite intersected in SE18 is interpreted to have been emplaced as a shallow intrusive body penecontemporaneously after the deposition of the

encompassing black mudstones of the Black Flag Group and may represent a section closer to the advancing front of the intrusion (McPhie et al., 1993, Busby-Spera and White, 1987, Kokelaar, 1982, White et al., 2000).

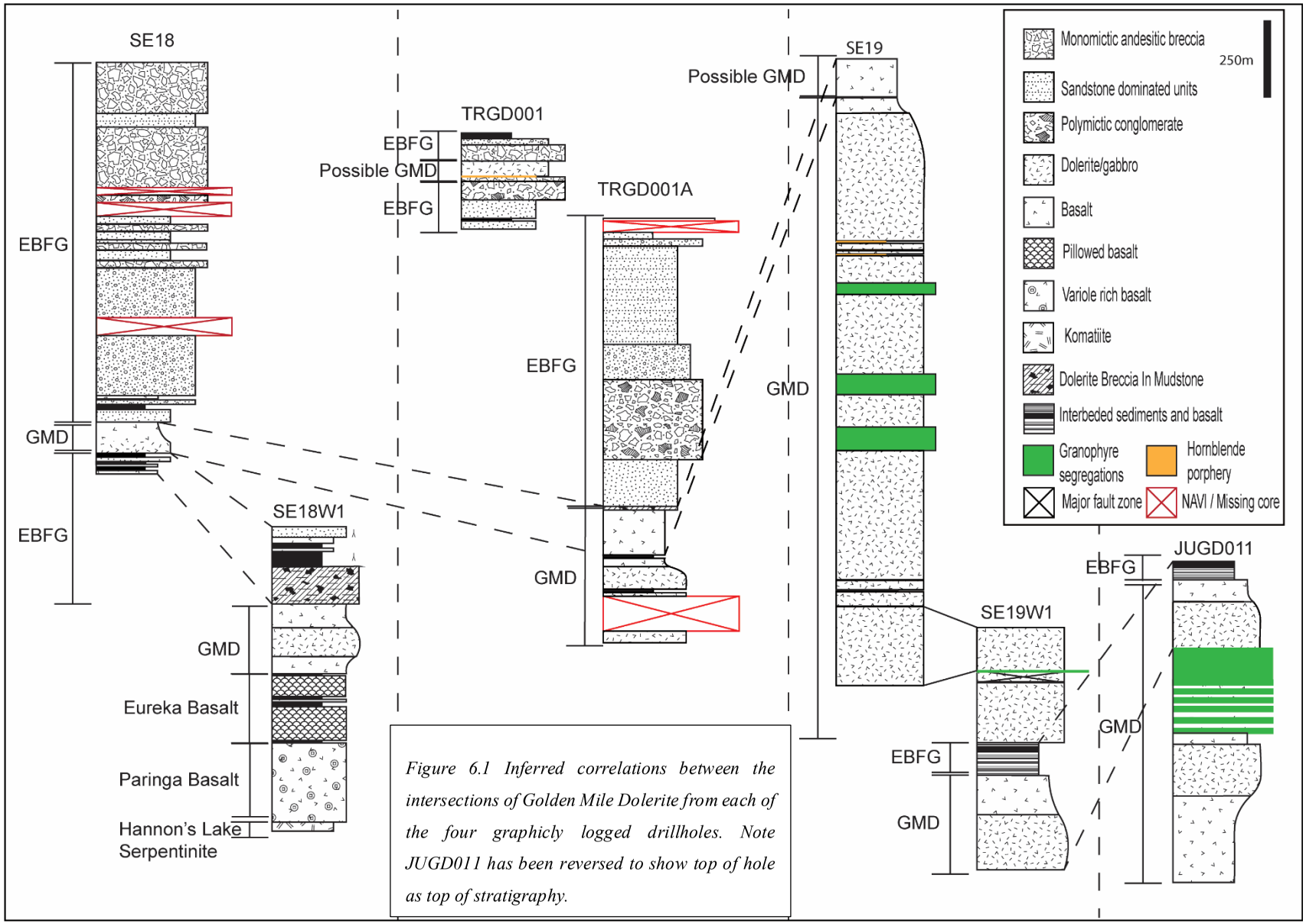

Figure 6.1 Inferred correlations between the intersections of Golden Mile Dolerite from each of the four graphicly logged drillholes. Note JUGD011 has been reversed to show top of hole as top of stratigraphy.

6.4.2 Evidence from SE19

The top contact between the Golden Mile Dolerite (Aberdare Dolerite sub-unit) and the sedimentary units of the Black Flag Group in SE19 is not present, however, SE19 displays an upper section of what appears to be approximately 50m of pillow-like structures (Fig. 4.10). No clear boundary between the dolerite and pillowed sections of the drill hole could be identified, with what appeared to be a gradational coarsening into dolerite. These pillows were unfortunately not sampled for geochemical analysis and as a result, it is unclear if they are related to the underlying Golden Mile Dolerite or one of the other pillowed units of the Kalgoorlie stratigraphy. It is also not clear if these structures are actually true pillows or if they represent the lobate contacts of a pillowed sill into possible unconsolidated wet sediment as is in line with observations made in the other three drill holes (Kano, 1991, McPhie et al., 1993). Alternately if these structures represent true pillows and could be related to the Golden Mile Dolerite (Aberdare Dolerite) then it may represent a localised extrusive section of the Golden Mile Dolerite. Although widely absent from the literature these basaltic "pillows" align with mapped unspecified basalts at the contact between the Golden Mile Dolerite (Aberdare dolerite) and Black Flag Group (Vielreicher et al., 2010). The situation is further complicated as bedrock at the site is not accessible due to the tailings pile which overlies the site.

6.4.3. Evidence from TRGD001

TRGD001 intersects roughly the same section of the Golden Mile Dolerite (Aberdare Dolerite) as SE19 and gives possible insights into the possible pillows mentioned previously. TRGD001 intersects a relatively thin (approx. 50m) dolerite body at an unusual position within the stratigraphy (200-250m) when compared to the other drill holes (Fig 6.1). This body occurs between polymictic conglomerates and andesitic mass flow breccias of the Black Flag Group rather than the basal thick mudstone units as seen in SE18 (Fig 6.1). The nature of this body is unclear as the core hosting the upper contact is abruptly missing and the bottom contact has been destroyed by a later hornblende porphyry intrusion. Without these contacts the emplacement of this body cannot accurately be determined. The top of the main dolerite body in this hole occurs much deeper in the hole (1345m) and is marked by a thin black mudstone bed overlain by turbidite sequences and volcaniclastic units (Fig 6.1). This overlying black mudstone unit contains angular randomly orientated basalt fragments

which are analogous to those found in SE18 (Fig. 4.4). The main basaltic body of this contact show clear chilled/possibly originally glassy margins near the contact with the mudstones, a feature which is largely absent in the other drill holes (Fig. 4.4 E, F). The basaltic fragments of these breccias tend to be generally larger and "blockier" in shape when compared to other drill holes, while the contact shows an undulating shape. These breccias have been interpreted in the same way as in the previous holes as peperitic wet sediment interactions for the reasons described above (McPhie et al., 1993, Busby-Spera and White, 1987, Kokelaar, 1982, White et al., 2000). Unlike SE18, TRGD001 shows two internal mudstone beds which are up to 10m thick within the Dolerite body. These mudstones seem to separate the body into at least three subsections with the possibility of more as roughly 125m of the core is missing from the bottom subsection 1645 -1770 (Fig. 6.1). The upper subunit which shows the peperitic margin shows almost no textural change primarily as fine-grained basalt, while the lower two subunits show gradational changes from basalt/dolerite to gabbro. This difference may be the result of intense alteration masking true texture, however, the bottom contact of the upper subunit with its underlying mudstone did not show peperitic breccias. The origin of these three, separated basaltic to dolerite units may be related or possibly unrelated however without geochemical data it is unclear how they relate. The top sub-unit with a peperitic margin was clearly a syn-depositional intrusion, as in SE18, whereas the lower two subunits, which both coarsen into gabbro were also emplaced as intrusions, because lavas do not crystallise gabbroic centres. However, without peperitic margins, they could have been emplaced as syn- or post-depositional intrusions.

6.4.4. Evidence from JUGD011

The contact relationships of JUGD011 are poorly exposed with only the top contact with the Black Flag Group exposed at the end of the hole. The main dolerite body of this unit shows possible peperitic or hydrothermally brecciated contacts although the relationships are not clear. Thin basaltic bodies (1 to 10 cms thick) in the overlying Black Flag sediments, however, show sparse peperitic textures (Fig. 4.4C) similar to those described in the other drill holes, and are interpreted as apophyses from the top contact of the GMD

6.5. Geochemical data discussion

The current and widely accepted theory for the emplacement of the Golden Mile Dolerite involves the intrusion of a mafic basaltic-gabbroic sill into the black mudstones of the of the lower Black Flack Group (Gustafson and Miller, 1937, Travis et al., 1971). Common evidence cited for this involves the development of the 10-distinct internal geochemical and textural units of the Golden Mile Dolerite, which are interpreted to represent the in-situ differentiation of an intrusive sill (Travis et al., 1971). In addition to in-situ differentiation, the presence of multiple subsequent Fe rich magmatic injections has been suggested to be responsible for the production of the central geochemical units 6-8 (Travis et al., 1971, McCall, 1973). When compared to the geochemical data used in this study, the 10 units (excluding the bottom chilled margin unit 1) could be distinguished in JUGD011 (Fig. 5.4). In the two smaller intersections of Golden Mile Dolerite of SE18 (100-200m observed thickness), the expression of these chemical groups is less easy, because the geochemically differentiated central units (units 6-8) are absent (Fig. 5.4). The contrast in geochemical trends between the two drill holes is likely due to the difference in thickness. As JUGD011 intersects a much larger (observed apparent thickness of 1170m in drill core) continuous body, it is likely that these rocks would have taken much longer to cool when compared to the thinner bodies of SE18 (Fig. 6.1). The differences in the thickness between the two drill holes relate to the position that they were drilled, in that JUGD011 was drilled in a central thicker section adjacent to the Fimiston pit while SE18 intersects a distal limb (approximately 3km from JUGD011) of the dolerite body (Fig. 2.1). The faster cooling subunits of SE18 can explain the difference in observed units as this would suppress the amount of differentiation the bodies could experience (Marsh, 2015). The mafic bodies of SE18 show a similar gradational change from fine basaltic upper sections to coarse gabbroic/cumulate textures with a minor chilled basal basalt margin (Fig. 6.1). These bodies show geochemical trends similar to those seen in units 1-5 and 9-10 of JUGD011 (Fig. 5.4, 6.1). The formation of chilled top and bottom margins and the development of cumulate zones as seen in SE18 and JUGD011 suggest an intrusive setting (Marsh, 2015). Rocks of this composition (units 1-5, 9-10) are thought to represent the original magmatic intrusion while units 6-7 and 8 represent later magmatic pulses (McCall, 1973). The absence of units 6-8 in SE18 is difficult to attribute entirely to the thickness and lack of extensive differentiation. The lack of any of the chemically distinct magma associated with units 6-8

suggests that this distal section may not have experienced the later injections. This is supported by the associated sharp chemical boundary between units 5 and 6 seen in JUGD011 which is absent in SE18, this does not support a completely in situ differentiation of the Golden Mile Dolerite at this location (Marsh, 2015, Zavala et al., 2011).

6.6 Emplacement models

6.6.1 Three-pulse system

Figures 6.2 and 6.3 show a proposed model for the syn-depositional emplacement of the Golden Mile Dolerite in which the internal units are attributed to three separate magma injection pulses. It is suggested that the Golden Mile Dolerite intruded the Black Flag Group before the overlying mudstones had been lithified. This initial intrusion likely produced the peperitic margins (described above) while forming the top and bottom units (1-5 and 9-10) through in-situ fractional crystallization. This fractional crystallization is displayed by the formation of basal pyroxene cumulate units 2 and 3 observed in JUGD011 and the formation of basil cumulates seen in both of the larger intrusions of SE18 (Figure 6.1) (McCall, 1973, Travis et al., 1971). Subsequently the injection of a second Fe rich magmatic pulse is evident through the stark change in geochemistry across a relatively small 10m interval between units 5 and 6 (Fig. 5.4). This later magma pulse is interpreted to be the product of fractional crystallization within a separate magmatic chamber delivering pulses of more evolved magma to form units 6-7. These injections of melt may have had limited access to the to the entirety of the intrusive body, for example the contrast in geochemical trends between the thick sequence of JUGD011 and the thin bodies of SE18. As SE18 lacks the sharp geochemical contact between units 5 and 6, these intersections being interpreted as farther from the supposed feeder zone and closer to the advancing front of the intrusion, may have cooled more rapidly (although still forming cumulates). Complete cooling of the thinner intrusions may have reduced the accessibility for the later pulses while paired with the distance from the source they may not have been able to experience these later pulses. In contrast, at the location of JUGD011, being proximal to the suspected feeder zone and subsequently in a thicker part of the intrusion, it is more reasonable to assume that later pulses, if smaller in volume would be more likely to occur closer to the source.

The formation of the granophyric segregations if the 3 pulse model of (McCall, 1973) is assumed to be correct, suggests that the highly evolved magma which formed the granophyre was emplaced as third and final magmatic pulse into the system. This pulse likely formed in the same way as pulse 2 through fractional crystallization within a lower feeder chamber which was then injected into the system. The emplacement of the coarse granophyric segregations into the fine basalts is unlikely the result of internal differentiation with the rapid change in grainsize seeming to show an almost intrusive relationship. These are interpreted to be the result of the injection of these highly evolved melts into the semi-solidified basalts of unit 7 likely through the process of solidification front instability tears (Marsh, 2015) while the upper more massive granophyre is likely the result of pooling evolved material (McDougall, 1964, McDougall, 1962).

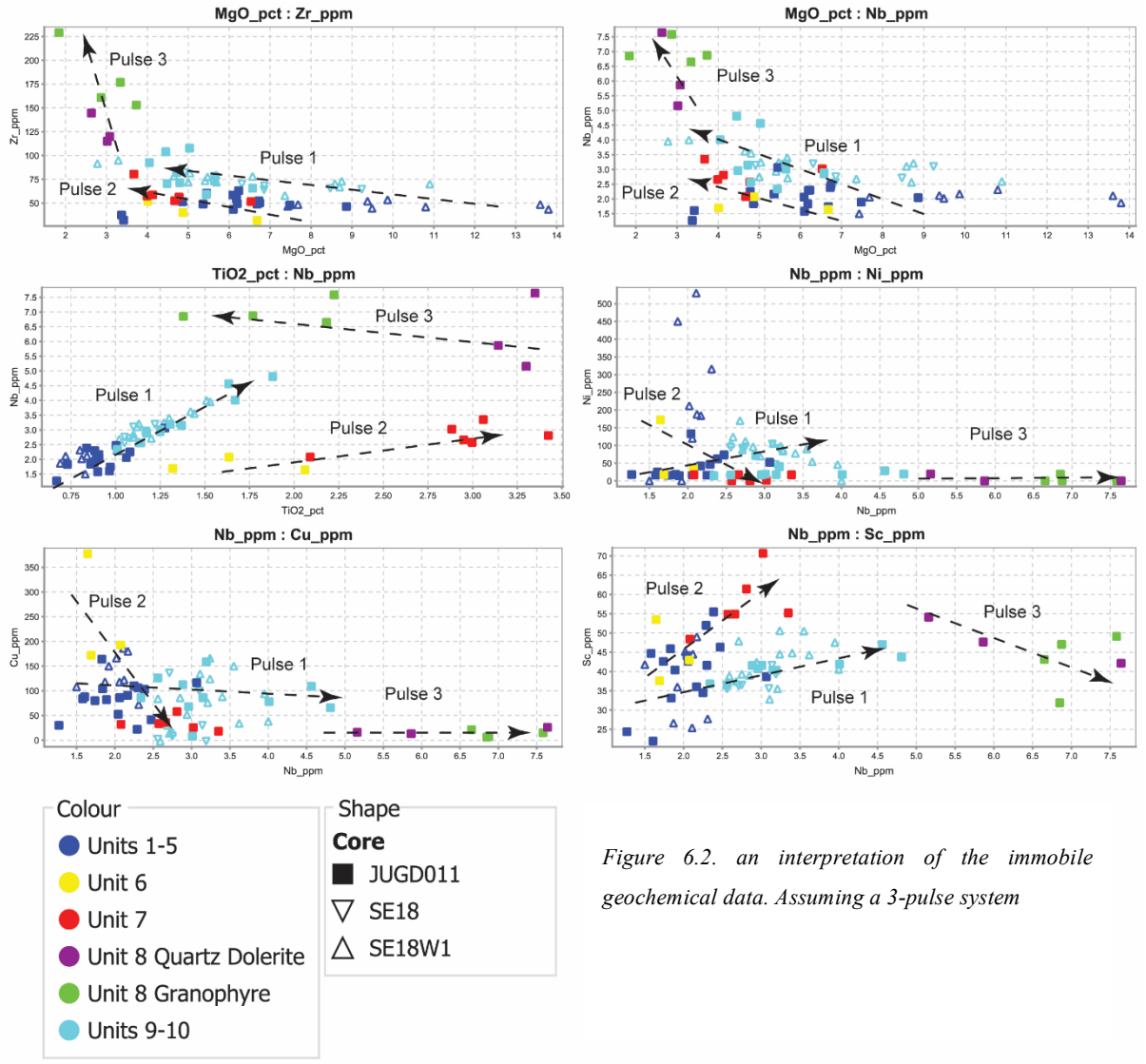

Figure 6.2. an interpretation of the immobile geochemical data. Assuming a 3-pulse system

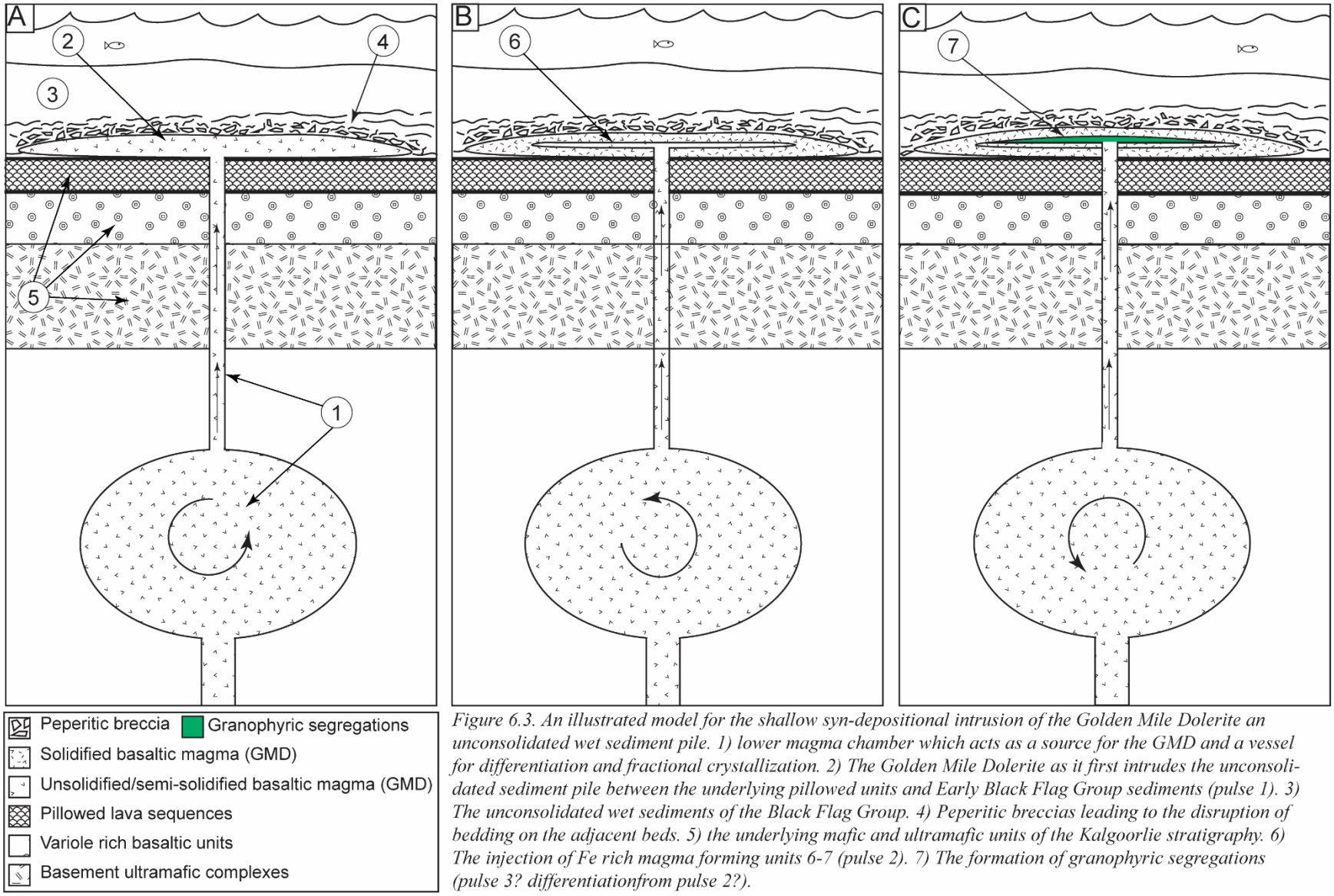

Figure 6.3. An illustrated model for the shallow syn-depositional intrusion of the Golden Mile Dolerite an unconsolidated wet sediment pile. 1) lower magma chamber which acts as a source for the GMD and a vessel for differentiation and fractional crystallization. 2) The Golden Mile Dolerite as it first intrudes the unconsolidated sediment pile between the underlying pillowed units and Early Black Flag Group sediments (pulse 1). 3) The unconsolidated wet sediments of the Black Flag Group. 4) Peperitic breccias leading to the disruption of bedding on the adjacent beds. 5) the underlying mafic and ultramafic units of the Kalgoorlie stratigraphy. 6) The injection of Fe rich magma forming units 6-7 (pulse 2). 7) The formation of granophyric segregations (pulse 3? differentiationfrom pulse 2?).

6.6.2 Two-pulse system

Alternatively, a two-pulse model could explain both the geochemical and physical observations for drill holes SE18 and JUGD011. For this model units 8A (Quartz Dolerite) and 8B (True Granophyre) are considered to be unrelated, in that 8A is suggested as the product of pulse 2 (units 6-7) and 8B is related as the product of differentiation for pulse 1 (units 1-5 and 9-10). These observations seem to align with geochemical trends (particularly Nb vs TiO_2) (Fig. 6.4.). Similar to the previously described three-pulse model, the emplacement of the first and largest pulse of magma responsible for units 1-5 and 9-10 was intruded into a wet, unconsolidated sediment pile of the lower black mudstones of the Black Flag Group. This is evident by the presence of peperite (Fig. 4.4) and fits within the suggested age ranges for the two units allowing for syn-depositional emplacement (Kokelaar, 1982, White et al., 2000, Kositcin et al., 2008, McPhie et al., 1993, Rasmussen et al., 2009). During the advanced stages of crystallization of the first magmatic pulse it is suggested that the second magmatic pulse intruded the crystal mush zone of the first pulse after a relatively large degree of fractional crystallization (Fig 6.4). The lack of granophyre in the upper unit 9 suggest that this original pulse may have cooled rapidly restricting the amount of in-situ differentiation that could have occurred (Zavala et al., 2011, Marsh, 2015). During this intrusion, the interstitial, evolved, groundmass melt trapped within the crystalizing framework was purged to a higher position within the magmatic body through mush flow fractionation (Marsh, 2015). The second magmatic pulse then begins to fractionate into an upper solidification front at the bottom of unit 9 forming the high Ti quartz dolerites of unit 8 (possibly through incorporation of evolved material?) as well as the lower units 6 and 7. The lower coarse grained unit 6 is interpreted as a product of fractional crystallisation and settling leaving the finer grained unit 7 which would agree with the increase in elements from the top of unit 7 to the bottom of unit 6 seen in downhole geochemistry (Marsh, 2015) (Figure 5.4.). alternatively, similar coarse grained basal units of the Ferrar Dolerite, Antarctica have been interpreted by Zavala et al. (2011) to possibly represent a crystal rich intrusion, however, this is unclear in the GMD. The morphology of this body is assumed to be as a domed laccolith, due to the variation in thickness observed form the interpreted central/ near feeder zone of JUGD011 compared to distal exposures seen in SE18. This would allow for the pooling of the granophyric material towards the upper sections with the roof lifting through the formation of the more massive granophyric

segregations/quartz dolerites seen in JUGD011 (Fig. 4.8) (Michaut, 2011). The thin granophyric segregations within the fine basalts of unit 7 in JUGD011 for this model have been related to possible solidification front instability leading to the detachment and or localised delamination of sections of the solidification front leading to the mixing and isolation of felsic melt segregations (Marsh, 2015, Marsh, 2002, Zavala et al., 2011).

The 2-pulse system is the preferred model for this study for several reasons. These include the what is interpreted as a better geochemical match showing two magma pulses rather than the previously suggested 3 or more pulse system (McCall, 1973, Travis et al., 1971). This is supported by the top of the secondary pulse units in the form of the unit 8A quartz dolerites overlying the true granophyric zones, interpreted as the end product of the primary pulse and not the product of a later granophyric intrusion (Fig. 6.4). there are also issues with the emplacement of a granophyric intrusion into the late stages of the sill due its viscus nature (Marsh, 2015)

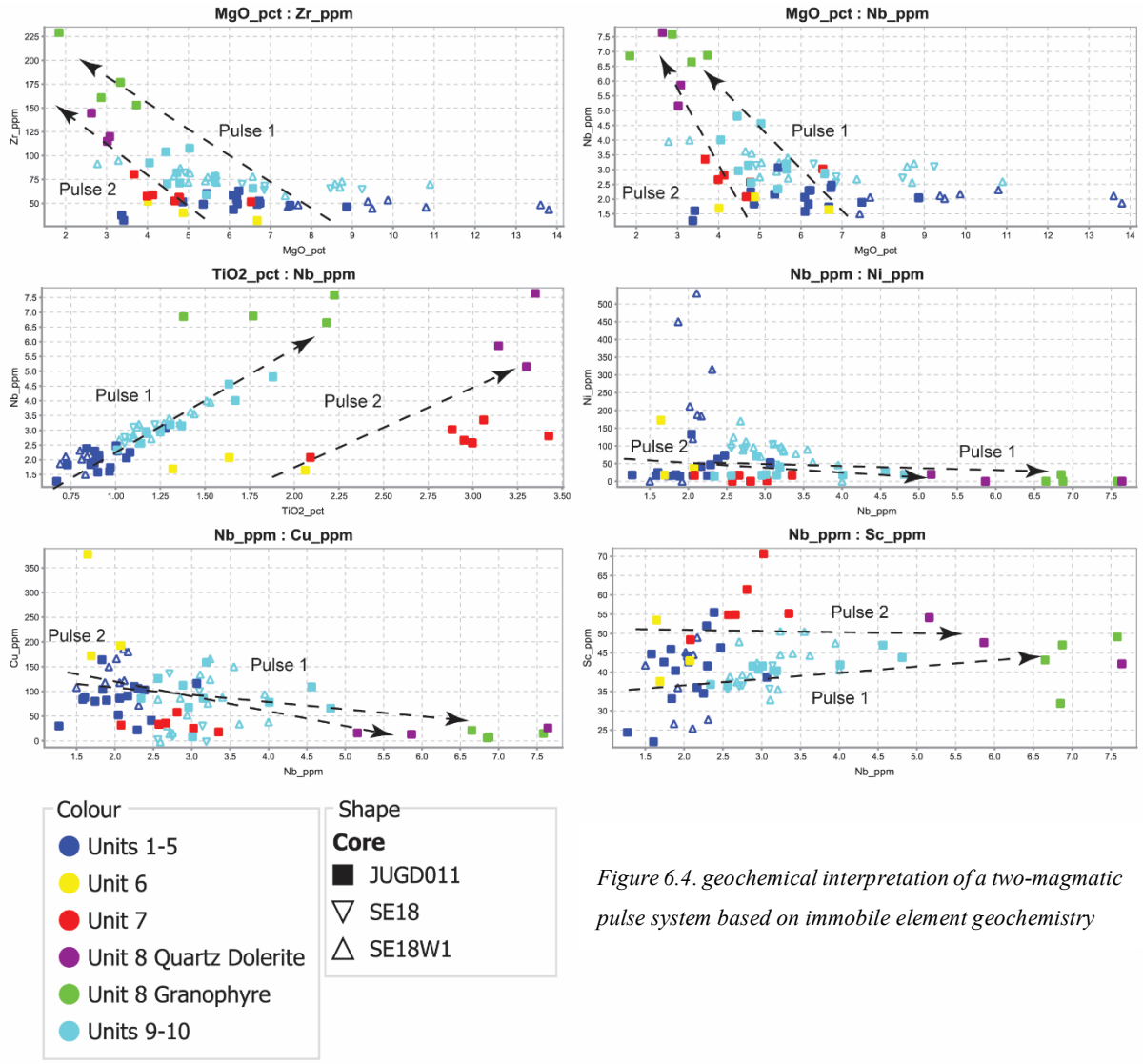

Figure 6.4. geochemical interpretation of a two-magmatic pulse system based on immobile element geochemistry

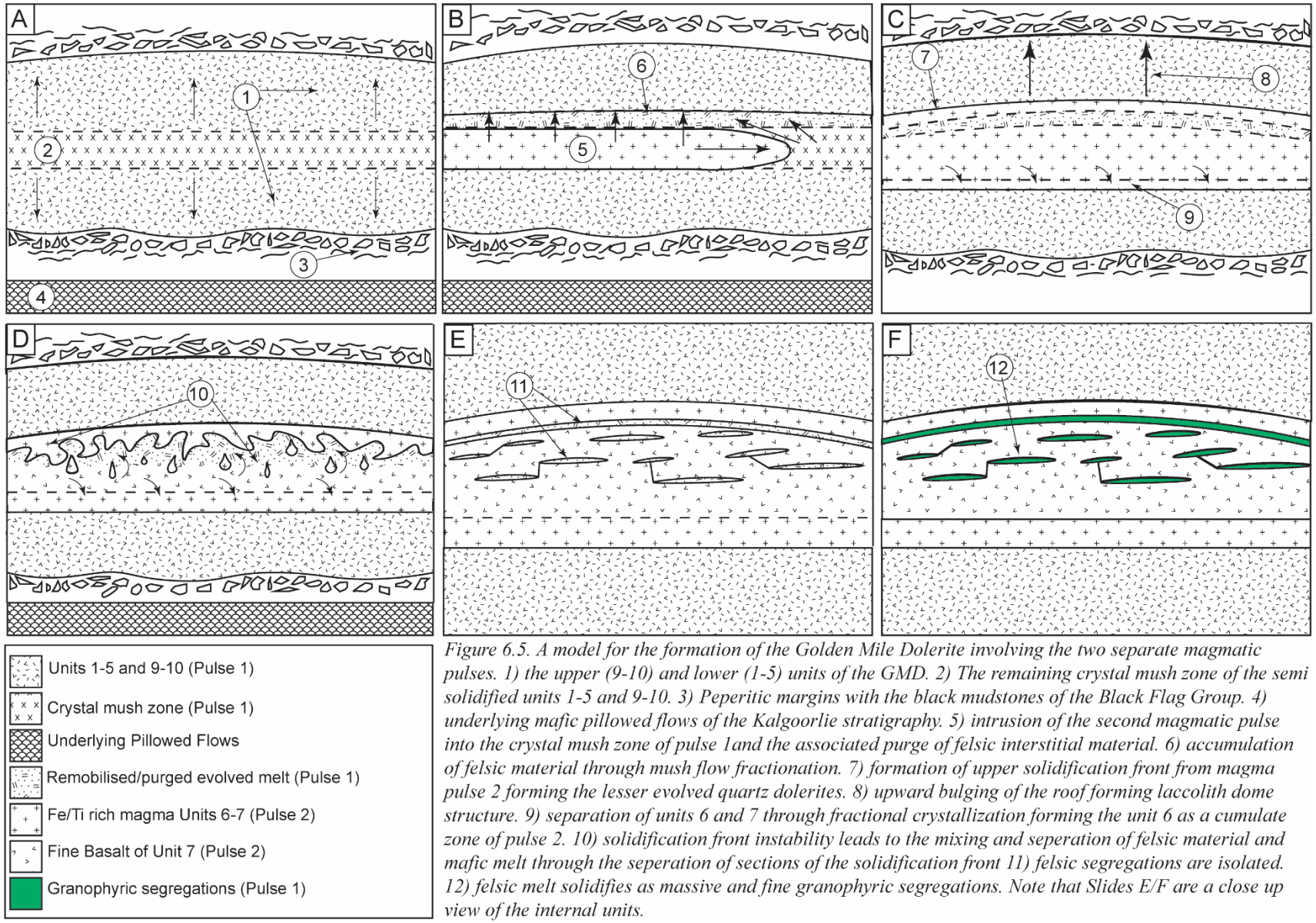

Figure 6.5. A model for the formation of the Golden Mile Dolerite involving the two separate magmatic pulses. 1) the upper (9-10) and lower (1-5) units of the GMD. 2) The remaining crystal mush zone of the semi solidified units 1-5 and 9-10. 3) Peperitic margins with the black mudstones of the Black Flag Group. 4) underlying mafic pillowed flows of the Kalgoorlie stratigraphy. 5) intrusion of the second magmatic pulse into the crystal mush zone of pulse 1and the associated purge of felsic interstitial material. 6) accumulation of felsic material through mush flow fractionation. 7) formation of upper solidification front from magma pulse 2 forming the lesser evolved quartz dolerites. 8) upward bulging of the roof forming laccolith dome structure. 9) separation of units 6 and 7 through fractional crystallization forming the unit 6 as a cumulate zone of pulse 2. 10) solidification front instability leads to the mixing and seperation of felsic material and mafic melt through the seperation of sections of the solidification front 11) felsic segregations are isolated. 12) felsic melt solidifies as massive and fine granophyric segregations. Note that Slides E/F are a close up view of the internal units.

7.0 Conclusions

- A geological and geochemical study was conducted to investigate the method of emplacement for the Golden Mile Dolerite. From these observations, a number of conclusions can be drawn:
- Crosscutting and interfingering relationships on many large dolerite bodies and smaller basaltic apophyses related to Golden Mile Dolerite suggest that it had an intrusive origin.
- Peperitic margins encountered on the top and bottom contacts of these bodies suggest that the Golden Mile Dolerite was emplaced as a high level syn-depositional intrusion.
- Geochemical data suggest that the formation of the Golden Mile Dolerite involved at least two magmatic pulses.

7.1. Further study

The following are recommended to further clarify the physical and chemical architecture of the Golden Mile Dolerite:

- A detailed geochemical survey of the thinner, distal sections of the Golden Mile Dolerite eg., SE18 to determine if the Fe/Ti enriched central units are truly absent or missed through insufficient sampling.
- Investigate more Drill holes which intersect the Golden Mile Dolerite to determine if the peperitic margins observed in this study are perversive across the whole of the body.
- Further investigation into the possible pillow-like features observed in SE19 with geochemical sampling to determine if they are related to the Golden Mile Dolerite. In addition, comparing these textures to other drillholes which intersect the same section of Golden Mile Dolerite (Aberdare Dolerite) would give insight into the nature of these features.

8.0. References

BARNES, S. J., VAN KRANENDONK, M. J. & SONNTAG, I. 2012. Geochemistry and tectonic setting of basalts from the Eastern Goldfields Superterrane. *Australian Journal of Earth Sciences,* 59**,** 707-735.

BATEMAN, R., COSTA, S., SWE, T. & LAMBERT, D. 2001. Archaean mafic magmatism in the Kalgoorlie area of the Yilgarn Craton, Western Australia: a geochemical and Nd isotopic study of the petrogenetic and tectonic evolution of a greenstone belt. *Precambrian Research,* 108**,** 75-112.

BLEWETT, R., CZARNOTA, K. & HENSON, P. 2010. Structural-event framework for the eastern Yilgarn Craton, Western Australia, and its implications for orogenic gold. *Precambrian Research,* 183**,** 203-229.

BLEWETT, R. S., CASSIDY, K. F., CHAMPION, D. C., HENSON, P. A., GOLEBY, B. S., JONES, L. & GROENEWALD, P. B. 2004. The Wangkathaa Orogeny: an example of episodic regional 'D2'in the late Archaean Eastern Goldfields Province, Western Australia. *Precambrian Research,* 130**,** 139-159.

BUSBY-SPERA, C. J. & WHITE, J. D. L. 1987. Variation in peperite textures associated with differing host-sediment properties. *Bulletin of Volcanology,* 49**,** 765-776.

CALDER, E. S., LAVALLÉE, Y., KENDRICK, J. E. & BERNSTEIN, M. 2015. Lava dome eruptions. *The Encyclopedia of Volcanoes (Second Edition).* Elsevier.

CASSIDY, K., CHAMPION, D., KRAPEZ, B., BARLEY, M., BROWN, S., BLEWETT, R., GROENEWALD, P. & TYLER, I. 2006. A revised geological framework for the Yilgarn Craton, Western Australia. *Geological Survey of Western Australia, Record,* 8.

CASSIDY, K., CHAMPION, D., MUHLING, J. & KNOX-ROBINSON, C. 2004. Crustal evolution of the Yilgarn Craton from Nd isotopes and granite geochronology: implications for metallogeny. *SEG***,** 317-320.

CHADWICK, W., CLAGUE, D., EMBLEY, R., PERFIT, M., BUTTERFIELD, D., CARESS, D., PADUAN, J., MARTIN, J. F., SASNETT, P. & MERLE, S. 2013. The 1998 eruption of Axial Seamount: New insights on submarine lava flow emplacement from high‐resolution mapping. *Geochemistry, Geophysics, Geosystems,* 14**,** 3939-3968.

CHAMPION, D. & CASSIDY, K. 2007. An overview of the Yilgarn Craton and its crustal evolution. *Geoscience Australia Record,* 14**,** 8-13.

CHAMPION, D. C. & SHERATON, J. W. 1997. Geochemistry and Nd isotope systematics of Archaean granites of the Eastern Goldfields, Yilgarn Craton, Australia: implications for crustal growth processes. *Precambrian Research,* 83**,** 109-132.

CLAGUE, D. A., DREYER, B. M., PADUAN, J. B., MARTIN, J. F., CHADWICK, W. W., CARESS, D. W., PORTNER, R. A., GUILDERSON, T. P., MCGANN, M. L. & THOMAS, H. 2013. Geologic history of the summit of Axial Seamount, Juan de Fuca Ridge. *Geochemistry, Geophysics, Geosystems,* 14**,** 4403-4443.

CLAOUÉ-LONG, J., COMPSTON, W. & COWDEN, A. 1988. The age of the Kambalda greenstones resolved by ion-microprobe: implications for Archaean dating methods. *Earth and Planetary Science Letters,* 89**,** 239-259.

CZARNOTA, K., CHAMPION, D., GOSCOMBE, B., BLEWETT, R., CASSIDY, K., HENSON, P. & GROENEWALD, P. 2010. Geodynamics of the eastern Yilgarn Craton. *Precambrian Research,* 183**,** 175-202.

DIMROTH, E., COUSINEAU, P., LEDUC, M. & SANSCHAGRIN, Y. 1978. Structure and organization of Archean subaqueous basalt flows, Rouyn–Noranda area, Quebec, Canada. *Canadian Journal of Earth Sciences,* 15**,** 902-918.

FLETCHER, I., DUNPHY, J., CASSIDY, K. & CHAMPION, D. 2001. Compilation of SHRIMP U–Pb geochronological data, Yilgarn Craton, Western Australia, 2000–2001. *Geoscience Australia, Record,* 47**,** 111.

FOSTER, J. & LAMBERT, D. Coupled Re-Os isotope and fluid dynamic constraints on the genesis of Archaean komatiite-hosted Fe-Ni-Cu (PGE) deposits. Geological Society of Australia Abstracts, 1996. 147.

FUNDIS, A. T., SOULE, S., FORNARI, D. & PERFIT, M. 2010. Paving the seafloor: Volcanic emplacement processes during the 2005‐2006 eruptions at the fast spreading East Pacific Rise, 9 50′ N. *Geochemistry, Geophysics, Geosystems,* 11.

GOLDING, L. Y. 1985. The nature of the Golden Mile Dolerite south‐east of Kalgoorlie, Western Australia. *Australian Journal of Earth Sciences,* 32**,** 55-63.

GREEN, T., BLUNDY, J., ADAM, J. & YAXLEY, G. 2000. SIMS determination of trace element partition coefficients between garnet, clinopyroxene and hydrous basaltic liquids at 2–7.5 GPa and 1080–1200 C. *Lithos,* 53**,** 165-187.

GUSTAFSON, J. K. & MILLER, F. 1937. Kalgoorlie geology re-interpreted. *Economic Geology,* 32**,** 285-317.

HANSON, R. B. 1995. The hydrodynamics of contact metamorphism. *Geological Society of America Bulletin,* 107**,** 595-611.

HARRIS, A. J. & ROWLAND, S. K. 2015. Lava flows and rheology. *The Encyclopedia of Volcanoes (Second Edition).* Elsevier.

HAYMAN, P. C., THÉBAUD, N., PAWLEY, M. J., BARNES, S. J., CAS, R. A., AMELIN, Y., SAPKOTA, J., SQUIRE, R. J., CAMPBELL, I. H. & PEGG, I. 2015. Evolution of a∼ 2.7 Ga large igneous province: a volcanological, geochemical and geochronological study of the Agnew Greenstone Belt, and new regional correlations

for the Kalgoorlie Terrane (Yilgarn Craton, Western Australia). *Precambrian Research,* 270**,** 334-368.

HENRICH, R. & HÜNEKE, H. 2011. Hemipelagic advection and periplatform sedimentation. *Developments in sedimentology.* Elsevier.

HÜNEKE, H. & HENRICH, R. 2011. Pelagic sedimentation in modern and ancient oceans. *Developments in sedimentology.* Elsevier.

KANO, K. 1991. Miocene pillowed sills in the Shimane Peninsula, SW Japan. *Journal of Volcanology and Geothermal Research,* 48**,** 359-366.

KOKELAAR, B. P. 1982. Fluidization of wet sediments during the emplacement and cooling of various igneous bodies. *Journal of the Geological Society,* 139**,** 21-33.

KOSITCIN, N., BROWN, S. J., BARLEY, M. E., KRAPEŽ, B., CASSIDY, K. F. & CHAMPION, D. C. 2008. SHRIMP U-Pb zircon age constraints on the Late Archaean tectonostratigraphic architecture of the Eastern Goldfields superterrane, Yilgarn craton, Western Australia. *Precambrian Research,* 161**,** 5-33.

KRAPEZ, B., BROWN, S., HAND, J., BARLEY, M. & CAS, R. 2000. Age constraints on recycled crustal and supracrustal sources of Archaean metasedimentary sequences, Eastern Goldfields Province, Western Australia: evidence from SHRIMP zircon dating. *Tectonophysics,* 322**,** 89-133.

KRAPEŽ, B. & HAND, J. L. 2008. Late Archaean deep-marine volcaniclastic sedimentation in an arc-related basin: the Kalgoorlie Sequence of the Eastern Goldfields Superterrane, Yilgarn Craton, Western Australia. *Precambrian Research,* 161**,** 89-113.

LEEDER, M. R. 2009. *Sedimentology and sedimentary basins: from turbulence to tectonics*, John Wiley & Sons.

LESHER, C. & ARNDT, N. 1995. REE and Nd isotope geochemistry, petrogenesis and volcanic evolution of contaminated komatiites at Kambalda, Western Australia. *Lithos,* 34**,** 127-157.

LOWE, D. R. 1982. Sediment gravity flows: II Depositional models with special reference to the deposits of high-density turbidity currents. *Journal of Sedimentary Research,* 52.

MAITRE, L. 1989. A classification of igneous rocks and glossary of terms. *Recommendations of the international union of geological sciences subcommission on the systematics of igneous rocks,* 193.

MARSH, B. D. 2002. On bimodal differentiation by solidification front instability in basaltic magmas, part 1: basic mechanics. *Geochimica et Cosmochimica Acta,* 66**,** 2211-2229.

MARSH, B. D. 2015. Magma chambers. *The Encyclopedia of Volcanoes (Second Edition).* Elsevier.

MCCALL, G. 1973. Geochemical characteristics of some Archaean greenstone suites of the Yilgarn structural province, Australia. *Chemical Geology,* 11**,** 243-269.

MCDOUGALL, I. 1962. Differentiation of the Tasmanian dolerites: Red Hill dolerite-granophyre association. *Geological Society of America Bulletin,* 73**,** 279-316.

MCDOUGALL, I. 1964. Differentiation of the great lake dolerite sheet, Tasmania. *Journal of the Geological Society of Australia,* 11**,** 107-132.

MCPHIE, J. 1993. *Volcanic textures: a guide to the interpretation of textures in volcanic rocks*.

MCPHIE, J. & CAS, R. 2015. Volcanic Successions Associated with Ore Deposits: Facies Characteristics and Ore–Host Relationships. *The Encyclopedia of Volcanoes (Second Edition).* Elsevier.

MCPHIE, J., DOYLE, M., ALLEN, R. L., ALLEN, R., DEPOSIT, U. O. T. C. F. O. & STUDIES, E. 1993. *Volcanic Textures: A Guide to the Interpretation of Textures in Volcanic Rocks*, Centre for Ore Deposit and Exploration Studies, University of Tasmania.

MEIBURG, E. & KNELLER, B. 2010. Turbidity currents and their deposits. *Annual Review of Fluid Mechanics,* 42**,** 135-156.

MICHAUT, C. 2011. Dynamics of magmatic intrusions in the upper crust: Theory and applications to laccoliths on Earth and the Moon. *Journal of Geophysical Research: Solid Earth,* 116.

MILLS, P. C. 1983. Genesis and diagnostic value of soft-sediment deformation structures—a review. *Sedimentary Geology,* 35**,** 83-104.

MORRIS, P. A. 1993. *Archaean mafic and ultramafic volcanic rocks, Menzies to Norseman, Western Australia*, Geological Survey of Western Australia.

MUELLER, A., HARRIS, L. & LUNGAN, A. 1988. Structural control of greenstone-hosted gold mineralization by transcurrent shearing: a new interpretation of the Kalgoorlie Mining District, Western Australia. *Ore Geology Reviews,* 3**,** 359-387.

MUELLER, A. G. 2015. Structure, alteration, and geochemistry of the Charlotte quartz vein stockwork, Mt Charlotte gold mine, Kalgoorlie, Australia: time constraints, down-plunge zonation, and fluid source. *Mineralium Deposita,* 50**,** 221-244.

MULDER, T., HÜNEKE, H. & VAN LOON, A. 2011. Progress in deep-sea sedimentology. *Developments in Sedimentology.* Elsevier.

NIXON, D., HESFORD, C., FITZGERALD, M. & LISTER, G. Relative timing of gold mineralization within the Kalgoorlie camp. Gold14@ Kalgoorlie—International Symposium. Curtin University, KalgoorlieAustralian Institute of Geoscientists, Australia, 2014. 97-98.

O'CONNOR-PARSONS, T. & STANLEY, C. R. 2007. Downhole lithogeochemical patterns relating to chemostratigraphy and igneous fractionation processes in the Golden Mile dolerite, Western Australia. *Geochemistry: Exploration, Environment, Analysis,* 7**,** 109-127.

RASMUSSEN, B., MUELLER, A. G. & FLETCHER, I. R. 2009. Zirconolite and xenotime U–Pb age constraints on the emplacement of the Golden Mile Dolerite sill and gold mineralization at the Mt Charlotte mine, Eastern Goldfields Province, Yilgarn Craton, Western Australia. *Contributions to Mineralogy and Petrology,* 157**,** 559-572.

SAID, N. & KERRICH, R. 2009. Geochemistry of coexisting depleted and enriched Paringa Basalts, in the 2.7 Ga Kalgoorlie Terrane, Yilgarn Craton, Western Australia: evidence for a heterogeneous mantle plume event. *Precambrian Research,* 174**,** 287-309.

SAID, N. & KERRICH, R. 2010. Elemental and Nd-isotope systematics of the Upper Basalt Unit, 2.7 Ga Kambalda Sequence: Quantitative modeling of progressive crustal contamination of plume asthenosphere. *Chemical Geology,* 273**,** 193-211.

SAID, N., KERRICH, R. & GROVES, D. 2010. Geochemical systematics of basalts of the Lower Basalt Unit, 2.7 Ga Kambalda Sequence, Yilgarn craton, Australia: plume impingement at a rifted craton margin. *Lithos,* 115**,** 82-100.

SCHULTEN, I., MOSHER, D. C., KRASTEL, S., PIPER, D. J. W. & KIENAST, M. 2018. Surficial sediment failures due to the 1929 Grand Banks Earthquake, St Pierre Slope. *Geological Society, London, Special Publications,* 477.

SQUIRE, R. J., ALLEN, C. M., CAS, R. A. F., CAMPBELL, I. H., BLEWETT, R. S. & NEMCHIN, A. A. 2010. Two cycles of voluminous pyroclastic volcanism and sedimentation related to episodic granite emplacement during the late Archean: Eastern Yilgarn Craton, Western Australia. *Precambrian Research,* 183**,** 251-274.

SQUIRE, R. J., CAS, R. A. F., CLOUT, J. M. F. & BEHETS, R. 1998. Volcanology of the Archaean Lunnon Basalt and its relevance to nickel sulfide‐bearing trough structures at Kambalda, Western Australia. *Australian Journal of Earth Sciences,* 45**,** 695-715.

SWAGER, C. 1989. Structure of Kalgoorlie Greenstones: Regional Deformation History and Implications for the Structural Setting of the Golden Mile Gold Deposits. *Report,* 25**,** 59-84.

SWAGER, C. P. 1997. Tectono-stratigraphy of late Archaean greenstone terranes in the southern Eastern Goldfields, Western Australia. *Precambrian Research,* 83**,** 11-42.

TOMICH, S. A new look at Kalgoorlie Golden Mile geology. Proceedings of the Australasian Institute of Mining and Metallurgy, 1974. 27-35.

TRAVIS, G., WOODALL, R. & BARTRAM, G. 1971. The geology of the Kalgoorlie goldfield. *Geol Soc Aust Spec Publ,* 3**,** 175-190.

UI, T., MATSUWO, N., SUMITA, M. & FUJINAWA, A. 1999. Generation of block and ash flows during the 1990–1995 eruption of Unzen Volcano, Japan. *Journal of Volcanology and Geothermal Research,* 89**,** 123-137.

VAN OTTERLOO, J., CAS, R. & R SCUTTER, C. 2015a. *The fracture behaviour of volcanic glass and relevance to quench fragmentation during formation of hyaloclastite and phreatomagmatism*.

VAN OTTERLOO, J., CAS, R. A. F. & SCUTTER, C. R. 2015b. The fracture behaviour of volcanic glass and relevance to quench fragmentation during formation of hyaloclastite and phreatomagmatism. *Earth-Science Reviews,* 151**,** 79-116.

VIELREICHER, N. M., GROVES, D. I. & MCNAUGHTON, N. J. 2016. The giant Kalgoorlie Gold Field revisited. *Geoscience Frontiers,* 7**,** 359-374.

VIELREICHER, N. M., GROVES, D. I., SNEE, L. W., FLETCHER, I. R. & MCNAUGHTON, N. J. 2010. Broad synchroneity of three gold mineralization styles in the Kalgoorlie gold field: SHRIMP, U-Pb, and 40Ar/39Ar geochronological evidence. *Economic Geology,* 105**,** 187-227.

WHITE, J. D. L., MCPHIE, J. & SKILLING, I. 2000. Peperite: a useful genetic term. *Bulletin of Volcanology,* 62**,** 65-66.

ZAVALA, K., LEITCH, A. M. & FISHER, G. W. 2011. Silicic segregations of the Ferrar Dolerite sills, Antarctica. *Journal of Petrology,* 52**,** 1927-1964.

RECORD 2019/7

A SYN-DEPOSITIONAL SILL INTRUSIVE MODEL FOR THE GOLDEN MILE DOLERITE, KALGOORLIE, WESTERN AUSTRALIA

McMann

This Record is published in digital format (PDF) and is available as a free download from the DMIRS website at <www.dmp.wa.gov.au/GSWApublications>.

Further details of geoscience products can be obtained by contacting:

Information Centre
Department of Mines, Industry Regulation and Safety
100 Plain Street
EAST PERTH WESTERN AUSTRALIA 6004
Phone: +61 8 9222 3459 Fax: +61 8 9222 3444
www.dmp.wa.gov.au/GSWApublications